UPPSALA
UNIVERSITET

Digital Comprehensive Summaries of Uppsala Dissertations from the Faculty of Science and Technology 1715

Ion pairing and Langmuir-like adsorption at aqueous surfaces studied by core-level spectroscopy

VICTOR EKHOLM

ACTA
UNIVERSITATIS
UPSALIENSIS
UPPSALA
2018

ISSN 1651-6214
ISBN 978-91-513-0432-8
urn:nbn:se:uu:diva-357369

Dissertation presented at Uppsala University to be publicly examined in Polhemsalen, Ångströmlaboratoriet, Lägerhyddsvägen 1, Uppsala, Friday, 19 October 2018 at 10:15 for the degree of Doctor of Philosophy. The examination will be conducted in English. Faculty examiner: Professor Markus Ammann (Paul Scherrer Institute).

Abstract
Ekholm, V. 2018. Ion pairing and Langmuir-like adsorption at aqueous surfaces studied by core-level spectroscopy. *Digital Comprehensive Summaries of Uppsala Dissertations from the Faculty of Science and Technology* 1715. 62 pp. Uppsala: Acta Universitatis Upsaliensis. ISBN 978-91-513-0432-8.

Surface-bulk equilibria for solutes in aqueous solutions are studied using X-ray Photoelectron Spectroscopy (XPS) with high surface and chemical sensitivity. In the first part, the results show a reduction of the biochemically relevant guanidinium ions' surface propensity with the addition of disodium sulphate due to ion pairing with the strongly hydrated sulphate ion, which could have implications for protein folding. Thereafter, the work considers amphiphilic organic compounds related to atmospheric science where the surface propensities, orientations at the surface and solute-solute and solute-solvent interactions are investigated. In the second part, two linear organic ions are investigated both as single solutes and in mixture. Both organic ions are surface enriched on their own and even more in the mixed solute solution. Due to hydrophobic expulsion of the alkyl chains, ion pairing between the organic ions and van der Waals interaction, the organic ions seem to assemble in clusters with their alkyl chains pointing out of the surface. The third part also covers linear organic compounds but one at a time probing the surface concentration as a function of bulk concentration. A Langmuir-like adsorption behavior was observed and Gibb's free energy of surface adsorption (ΔG_{Ads}) values were extracted. An empiric model for deriving values for ΔG_{Ads} is proposed based upon the seemingly linear change in ΔG_{Ads} per carbon when comparing alcohols of different chain lengths. The fourth part investigates the acid/base fraction at the surface as function of bulk pH. The most important factor for this fraction seems to be how the surface propensity varies with the charge state of the acid or base instead of a possible difference in pH or pK_a value at the surface. In the fifth part the oxygen K-edge of aqueous carbonate and bicarbonate is probed with the bulk-sensitive Resonant Inelastic X-ray Scattering (RIXS) technique.

Keywords: XPS, Surface, Aqueous, Liquid jet, Langmuir

Victor Ekholm, Department of Physics and Astronomy, Molecular and Condensed Matter Physics, Box 516, Uppsala University, SE-751 20 Uppsala, Sweden.

ISSN 1651-6214
ISBN 978-91-513-0432-8
urn:nbn:se:uu:diva-357369 (http://urn.kb.se/resolve?urn=urn:nbn:se:uu:diva-357369)

"This is insanity! No! This is scholarship!",
Shallan in Word of Radiance by Brandon Sanderson.

List of papers

This thesis is based on the following papers, which are referred to in the text by their Roman numerals.

I **Anomalous surface behavior of hydrated guanidinium ions due to ion pairing**
Victor Ekholm, Mario Vazdar, Philip E. Mason, Erik Bialik, Marie-Madeleine Walz, Gunnar Öhrwall, Josephina Werner, Jan-Erik Rubensson, Pavel Jungwirth and Olle Björneholm
Journal of Chemical Physics, **148** (14), art. no. 144508, DOI: 10.1063/1.5024348 (2018)

II **Strong Enrichment of Atmospherically Relevant Organic Ions at the Aqueous Interface: The Role of Ion Pairing and Cooperative Effects**
Victor Ekholm, Carl Caleman, Nicklas Bjärnhall Prytz, Marie-Madeleine Walz, Josephina Werner, Gunnar Öhrwall, Jan-Erik Rubensson and Olle Björneholm
Submitted

III **Surface propensity of atmospherically relevant carboxylates and alkyl ammonium ions studied by XPS : towards a building-block model of surface propensity based on Langmuir adsorption**
Victor Ekholm, Carl Caleman, Marie-Madeleine Walz, Josephina Werner, Gunnar Öhrwall, Jan-Erik Rubensson and Olle Björneholm
In manuscript

IV **Surface behavior of amphiphilies in aqueous solution: a comparison between different pentanol isomers**
Marie-Madeleine Walz, Carl Caleman, Josephina Werner, Victor Ekholm, Daniel Lundberg, Nønne L. Prisle, Gunnar Öhrwall and Olle Björneholm
Physical Chemistry Chemical Physics, **17**, 14036-14044 (2015)

V **Alcohols at the aqueous surface: chain length and isomer effects**
Marie-Madeleine Walz, Josephina Werner, Victor Ekholm, Nønne L. Prisle, Gunnar Öhrwall and Olle Björneholm
Physical Chemistry Chemical Physics, **18**, 6648 (2016)

VI **Shifted Equilibria of Organic Acids and Bases in the Aqueous Surface Region**
Josephina Werner, Ingmar Persson, Olle Björneholm, Delphine Kawecki, Clara-Magdalena Saak, Marie-Madeleine Walz, Victor Ekholm, Isaak Unger, Corina Valtl, Carl Caleman, Gunnar Öhrwall and Nønne L. Prisle
Physical Chemistry Chemical Physics,
DOI: 10.1039/C8CP01898G, (2018)

VII **Aqueous carbonate and bicarbonate ions studied by RIXS at the O K-edge**
Victor Ekholm, Johan Gråsjö, Minjie Dong, Olle Björneholm, Conny Såthe, Evanthia Chatzigeorgiou, Marcus Agåker, Yoshihisa Harada, Jun Miyawaki and Jan-Erik Rubensson
In manuscript

Reprints were made with permission from the publishers.

Extended bibliography

1. **Surface Behavior of Hydrated Guanidinium and Ammonium Ions: A Comparative Study by Photoelectron Spectroscopy and Molecular Dynamics.**
   Josephina Werner, Erik Wernersson, Victor Ekholm, Niklas Ottosson, Gunnar Öhrwall, Jan Heyda, Ingmar Persson, Johan Söderström, Pavel Jungwirth and Olle Björneholm
   Journal of Physical Chemistry B, **118**, 25: 7119-7127 (2014)

2. **Deeper Insight into Depth-Profiling of Aqueous Solutions Using Photoelectron Spectroscopy**
   Olle Björneholm, Josephina Werner, Niklas Ottosson, Gunnar Öhrwall, Victor Ekholm, Bernd Winter, Isaak Unger and Johan Söderström
   Journal of Physical Chemistry C, **118**, 50: 29333-29339 (2014)

3. **Acid-Base Speciation of Carboxylate Ions in the Surface Region of Aqueous Solutions in the Presence of Ammonium and Aminium Ions**
   Gunnar Öhrwall, Nønne L. Prisle, Niklas Ottosson, Josephina Werner, Victor Ekholm, Marie-Madeleine Walz and Olle Björneholm
   Journal of Physical Chemistry B, **119**, 10: 4033-4040 (2015)

4. **Anomalously strong two-electron one-photon X-ray decay transitions in CO caused by avoided crossing**
   Rafael C. Couto, Marco Guarise, Alessandro Nicolaou, Nicolas Jaouen, Gheorghe S Chiuzbăian, Jan Lüning, Victor Ekholm, Jan-Erik Rubensson, Conny Såthe, Franz Hennies, Victor Kimberg, Freddy F. Guimarães, Hans Ågren, Faris Gel'mukhanov, Loïc Journel and Marc Simon
   Scientific Reports, **6**, art. num. 20947 (2016)

5. **Coupled electron-nuclear dynamics in resonant $1\sigma \rightarrow 2\pi$ X-ray Raman scattering of CO molecules**
   Rafael C. Couto, Marco Guarise, Alessandro Nicolaou, Nicolas Jaouen, Gheorghe S. Chiuzbăian, Jan Lüning, Victor Ekholm, Jan-Erik Rubensson, Conny Såthe, Franz Hennies, Freddy F. Guimarães, Hans Ågren, Faris Gel'mukhanov, Loïc Journel, Marc Simon, and Victor Kimberg
   Physical Review A, **93**, 032510 (2016)

6. **Surface Partitioning in Organic-Inorganic Mixtures Contributes to the Size-Dependence of the Phase-State of Atmospheric Nanoparticles**
Josephina Werner, Maryam Dalirian, Marie-Madeleine Walz, Victor Ekholm, Ulla Wideqvist, Samuel J. Lowe, Gunnar Öhrwall, Ingmar Persson, Ilona Riipinen and Olle Björneholm
Environmental Science and Technology, **50** (14): 7434-7442 (2016)

7. **Ethanol Solvation in Water Studied on a Molecular Scale by Photoelectron Spectroscopy**
Ricardo R. T. Marinho, Marie-Madeleine Walz, Victor Ekholm, Gunnar Öhrwall, Olle Björneholm and Arnaldo Naves de Brito
Journal of Physical Chemistry B, **121** (33): 7916-7923 (2017)

Comments on my personal participation

As many things in life, teamwork is always the best way forward in my opinion. The work presented in this thesis is certainly a joint effort and I'm grateful for the help and contribution from everyone involved. In all presented papers, I have participated in the experimental work, discussions and been involved in the writing process in different degrees. In the papers in which I have been the first author I also planned the experiments and preformed the analysis. In paper II, I analyzed parts of the MD-simulations as well.

Contents

1 Introduction and background 11

2 Important concepts 15
2.1 Ion pairing 15
2.2 Langmuir isotherm adsorption 16

3 XPS 19
3.1 Soft X-ray Core-Level Spectroscopy 19
3.2 Binding energies and what we can learn 21
3.3 Surface sensitivity and orientation 21
3.4 Normalized intensity and stability over time 23
3.5 Two layer model and surface enrichment factors 23
3.6 Measurements at MAX II 24

4 A few words about RIXS 27
4.1 Two(three?)-step model 27
4.2 One-step model 28
4.3 Detuning and vibrations 28
4.4 Dipole approximation, selection rules and polarization 29

5 Summary of papers 31
5.1 Ion pairing and surface effects (Paper I and II) 31
5.1.1 Salting in or salting out? (Paper I) 32
5.1.2 What happens at the surface when mixing two organic ions together? (Paper II) 34
5.2 Langmuir adsorption (Paper III-V) 39
5.2.1 Surface abundance 39
5.2.2 Orientation 40
5.2.3 Dehydration and binding energy shifts 42
5.2.4 An attempt to formulate a building block model for surface adsorption 42
5.3 Are the pH and the pK_a values at the surface different compared to the bulk? (Paper VI) 43
5.4 Protonation affecting electronic states of carbonate (Paper VII) 47

6 Conclusions and Outlook 51

7 Populärvetenskaplig sammanfattning 53

8 List of abbreviations 57
9 Acknowledgments 58
References 60

1. Introduction and background

Water in its many forms is as beautiful as it is interesting. In nature water partakes in one of the biggest cycles on Earth – the hydrological cycle. In this cycle, one can consider water starting its journey in its solid form, best known as snow or ice as in for example glaciers. Consider the fourth biggest glacier in Sweden, called Bårddejiegna, which in Sami means something like the glacier of stacking, in the national park Sarek in the very north of Sweden. During the summer months the glacier partly melts and the now liquid water flows through rippling rivers and shimmering lakes for miles and miles until it reaches the Baltic sea. Along the journey and later in the sea the water can evaporate and rise in its gaseous form to the atmosphere. It can then through condensation return to its liquid phase in the shape of droplets, also known as clouds when gathered in numbers. Under the right circumstances clouds could, during the winter months, driven by the wind release the water as snow over Bårddejiegna to let it once again grow.

Unfortunately, future trekkers will only be able to see Bårddejiegna from old photos due to the ever increasing mean temperature of the Earth causing the glaciers all over the globe to melt more and grow less. The commonly known reason for this is the increased global warming. It is well known that carbon dioxide (CO_2) affects the Earth's radiative balance – the net in and out flow of energy from the sun. One perhaps not as well known contributer to global warming are clouds which in some cases, depending of the composition and size of the droplets, have shown to either contribute with a net effect increasing or decreasing global warming. One of the largest sources of uncertainty are aerosols [1, 2], small droplets with a size $\lesssim 1\mu$m. In such small droplets the surface layer becomes more important as it both contributes to a more significant part of the volume and is the region in which the water uptake and evaporation takes place. However, water droplets in clouds do not only contain pure water but a large variety of organic and inorganic molecules and ions at different pH values which composition depends on where the aerosols were formed. For example, sea aerosols usually contains salts like NaCl and NaBr, organic compounds are commonly found in aerosols formed over forests and aerosols found over cites can contain compounds emitted from industry.

The composition and chemistry of aqueous surfaces can in general be quite different from the bulk [3, 4]. Some of the atmospherically relevant compounds described above are surface enriched already in solutions with low bulk concentrations and could possibly be very enriched in an environment

with other compounds competing for staying hydrated. Organic compounds have potential of being surface enriched as they often contain hydrophobic parts [5, 6, 7]. Surface enriched organic compounds can affect evaporation properties but also the chemistry at the water/air interface changing acid/base speciation [8], catalytic reactions with organics [9, 10] and local densities [11]. Inorganic ions are also interesting as they have the possibility of affecting other solutes 'surface propensity and have long been thought to not reside at or close to the interface, which we now know they do – see section 2.1 for a detailed discussion about ions at the interface.

The propensity of biomolecules to biologically relevant hydrophobic interfaces, for example between the cell fluid and macromolecules such as proteins or cell membranes, and how physiological parameters such as pH and inorganic ions related to the Hofmeister series affect this, are important issues for a molecular-scale understanding of some biological processes. The vapor side of the water-vapor interface acts a very hydrophobic surface, and the water surface is thus as a good model for hydrophobic interfaces, which has inspired studies of biomolecules at the aqueous surface [12, 13].

Aqueous solutions and their surfaces are, as discussed, important for many reasons and consequently a lot of effort has been made to develop and adjust tools to study both bulk and surface properties. For bulk studies there are both spectroscopic techniques (NMR, XAS, RIXS, IR, UV-VIS, HAXPES, etc) and scattering techniques (XRD, neutron diffraction, etc) available, while for surface studies tools like sum-frequency generation, surface-enhanced Raman spectroscopy, surface tension and X-ray Photoelectron Spectroscopy (XPS) can been used. There are also computational methods available, like classical molecular dynamics (MD) used both for bulk and surface studies or density functional theory calculations for smaller systems.

The experimental work in thesis is mainly based upon XPS studies, or Electron Spectroscopy for Chemical Analysis (ESCA) as is was called by Kai Siegbahn who was awarded the Nobel prize for developing this technique. XPS is a technique widely used in "homelabs" and is a standard tool at synchrotron facilities, used for studying solids, gases, clusters and liquids. It is suited to study properties like electronic structure but can also be used to investigate various dynamical phenomena as well as structure.

Since vacuum is a prerequisite for XPS studies, it is not straightforward to probe volatile samples. Liquids were first successfully probed with XPS when introduced as a liquid jet along with differential pumping by father and son, Kai and Hans Siegbahn with co workers [14]. The technique was later refined by Manfred Faubel et al. [15], who introduced higher speeds and smaller diameters of the liquid jet that led to reduced evaporation rates – a key development. Modern developments, like more sophisticated differential pumping schemes, have also been made in ambition to reach ambient pressures, for example Scienta Omicron's HIPP or Specs' NAP analyzer.

To probe real systems at ambient conditions are preferable, though even with better spectrometers there are some intrinsic limitations. Real atmospheric droplets contain many substances which makes it very tricky to disentangle the different mechanisms affecting the solutes with spectroscopic techniques as of today. Another example is proteins, where the many chemically inequivalent atoms makes it difficult to resolve the contribution from the different atoms spectroscopically. All systems investigated in this thesis are liquid samples, most of the aqueous solutions probed at a synchrotron with XPS in combination with a liquid jet or RIXS using a liquid cell. The probed systems have mostly been model systems of more complicated ones, related to atmospheric science or biochemistry but also systems interesting for basic chemistry. The hope for the future is of course to gradually understand some aspects of real systems with the help of model systems.

2. Important concepts

2.1 Ion pairing

Since ion pairing is a key concept in paper I and II the following section will give some background information on the topic. An ion in an aqueous solution usually attracts and affects the surrounding water due to its charge interacting with the dipole of the water molecules, creating a hydration shell around the ion. Depending on the amount of charge and size of the ion, the size and the number of hydration shells varies [16]. More highly charged ions such as the divalent SO_4^{2-} ion, may even have a second hydration shell [17]. One has to be careful when discussing bulk-properties since the fraction of "free" water decreases with increasing salt concentration in electrolyte solutions [18]. With ions interacting with the surrounding water it is not surprising that ions could interact with other ions in solution.

An ion pair can be defined as an association of ions with opposite charge in a solution, where they are associated during some time, with a distance shorter than a certain cutoff distance [19]. This can be described as an equilibrium between the ions in association and as free ions, where the life time can vary depending on the system. For example is the life time of an Na^+-Cl^- ions pair, in a 0.5 M NaCl solution, estimated to be about 20 ps [20]. Ion pairs can be classified into three different categories, illustrated in Figure 2.1. Either as a contact ion pair (CIP), where the ions are in contact, as a solvent-shared ion pair (SIP), where they share one water molecule or as a solvent-separated ion pair (2SIP), where they share two water molecules [21]. Ion pairs can be encountered in a large variety of systems – naturally occurring in for example biological systems and in the atmosphere [22, 21].

According to the classical Onsager-Samaras model, single ions should avoid aqueous surfaces [23], though later, both experimental and theoretical work have shown that ions can reside close to the interface [3]. Ions have even been shown to form cluster-like structures residing at interfaces at low bulk concentrations [21]. Inorganic ions that normally do not form ion pairs in the bulk have shown to form ion pairs at the surface [24, 25]. The closer the ions come to the surface the weaker is the local dielectric field from the surrounding water molecules, hence facilitating ion paring as the effective force between the ions increases.

There are many different experimental methods for studying ion pairs. While macroscopic methods like conductometry and potentiometry are well established with their respective limitations, diffraction methods are limited to study

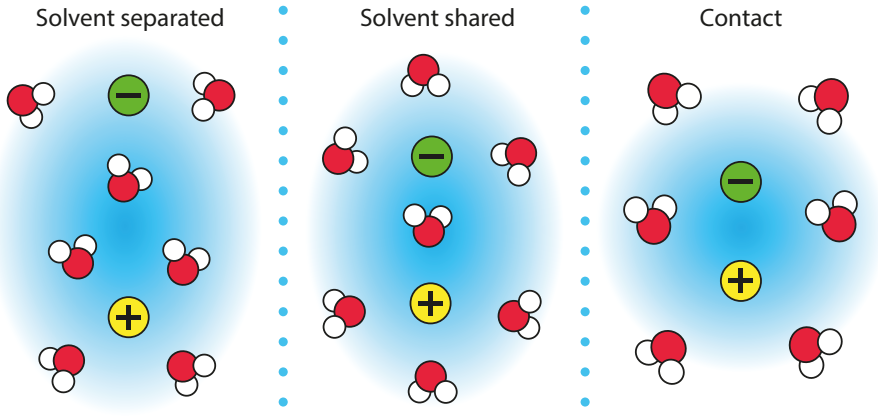

Figure 2.1. There are three main categories of ion pairing as depicted here. The ion pairs investigated in paper I and II are believed to be contact ion pairs.

structures, spectroscopy can (so far) only detect CIP but the, perhaps, most advantageous class of techniques are the relaxation methods. By first pumping and then probing how the system relaxes to its equilibrium state, it has been possible to discover SIPs and 2SIPs [19, 21]. To investigate ion pairs at surfaces, it is mainly either surface-enhanced Raman spectroscopy or sum frequency generation that has been used [21]. With paper I and II we show that X-ray photoelectron spectroscopy might also be an option for studying ion pairs at the aqueous surface.

2.2 Langmuir isotherm adsorption

Solutes in aqueous solutions are more or less abundant at the surface. As commonly known, oily compounds like olive oil in the vinaigrette or fuel for big ships are not soluble and tend to float on top of the water due to their lower density compared to water, but there are also miscible compounds that avoid the surface and are instead found in the bulk. Additionally, there is a whole spectrum of compounds that are soluble and can be found both in the bulk and the surface at the same time. With changing bulk concentration the surface abundance of the solute can also change and normally non-linearly. A similar mechanism was first described by Irving Langmuir – a model for to what degree gas molecules adsorb on a solid surface for a given temperature as a function of pressure [26]. This model assumes that there is no interaction between the gas particles, that there can be no more adsorption when the surface is fully covered as a monolayer and that the adsorption energy is independent of the degree of coverage. This model has been modified for adsorption of solutes at the surface of solutions [27, 28, 29, 30, 31], where the solute adsorbs on the surface (N_S) by replacing a solvent molecule at the surface (S_S). This

will be in equilibrium with the number of molecules in the bulk (N_B and S_B), as described by:

$$S_S + N_B \rightleftharpoons S_B + N_S \tag{2.1}$$

. The surface abundance, N_S is then modeled by:

$$N_S = \frac{N_{S,max} \cdot x_{bulk}}{x_{bulk} + (1 - x_{bulk}) \cdot e^{\Delta G/(R \cdot T)}} \tag{2.2}$$

, where $N_{S,max}$ is the maximum possible surface abundance at a bulk concentration where the surface is fully saturated, x_{bulk} is the molar fraction in the bulk, ΔG_{Ads} is the difference in Gibb's free energy between a solvated solute at the surface and one in the bulk, R is the molar constant and T is the temperature. The typical shape of Equation 2.2 can be seen in Figure 2.2 along with a schematic illustration of the surface-bulk equilibrium for different bulk concentrations. In real systems, solutes will probably interact with each other and the adsorption energy will also change as a function of surface abundance. Even if the necessary assumption for the Langmuir isotherm adsorption model are not completely fulfilled the model has worked reasonably well. In the cases where the interaction between the solutes becomes strong one could apply a more advanced model with different ΔG_{Ads} values for when the surface is little or highly saturated [32].

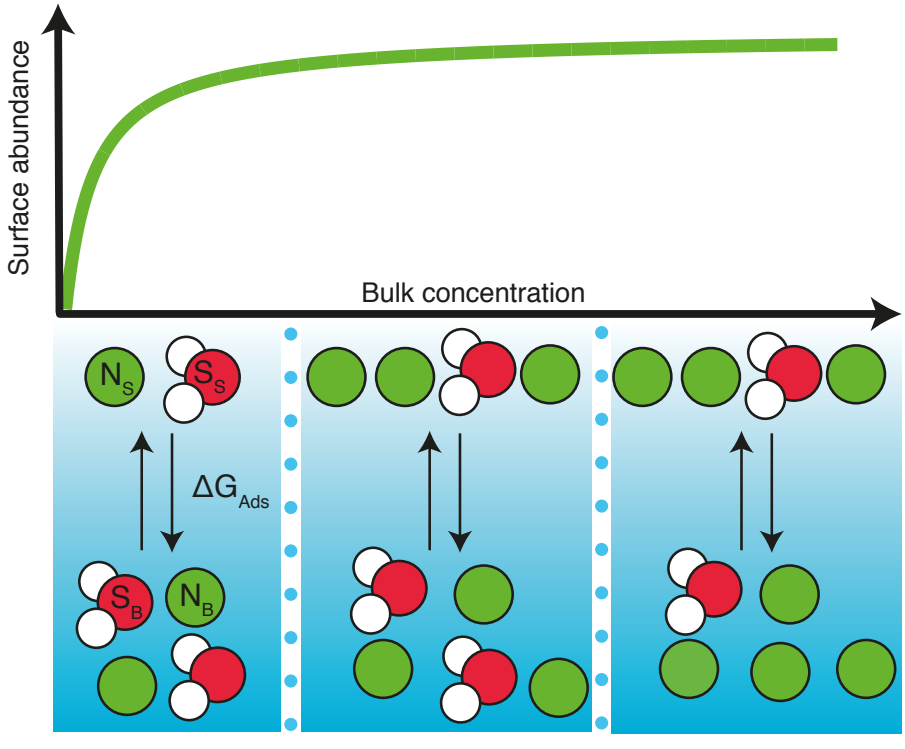

Figure 2.2. Schematic illustration of the surface-bulk equilibrium for the solute-solvent system and how the Langmuir-like surface saturation can look like.

3. XPS

Since X-ray Photoelectron Spectroscopy (XPS) is a technique with many details and has been described before (see for example ref. [33] and [34]), only some important aspects will be presented here.

3.1 Soft X-ray Core-Level Spectroscopy

Core-level XPS can be described as following. By knowing the energy of an incoming photon hν, and measuring the kinetic energy (KE) of an outgoing electron, we can hopefully gain information about the probed system. One of the most important concepts is the binding energy (BE) of electrons, which under certain conditions is given by,

$$\mathrm{BE} = \mathrm{h}\nu\text{-KE} \tag{3.1}$$

. In other words, one could interpret the BE of the electron to be the minimum energy needed for the electron to leave the system. After the core hole has been created, the surrounding electron cloud adapts fast enough to affect the outgoing electron and the BE. Though other, slower, relaxation processes can occur through different pathways. As long as the emitted electron is fast enough it will not be affected by for example Auger decay or geometrical changes – this is a common assumption.

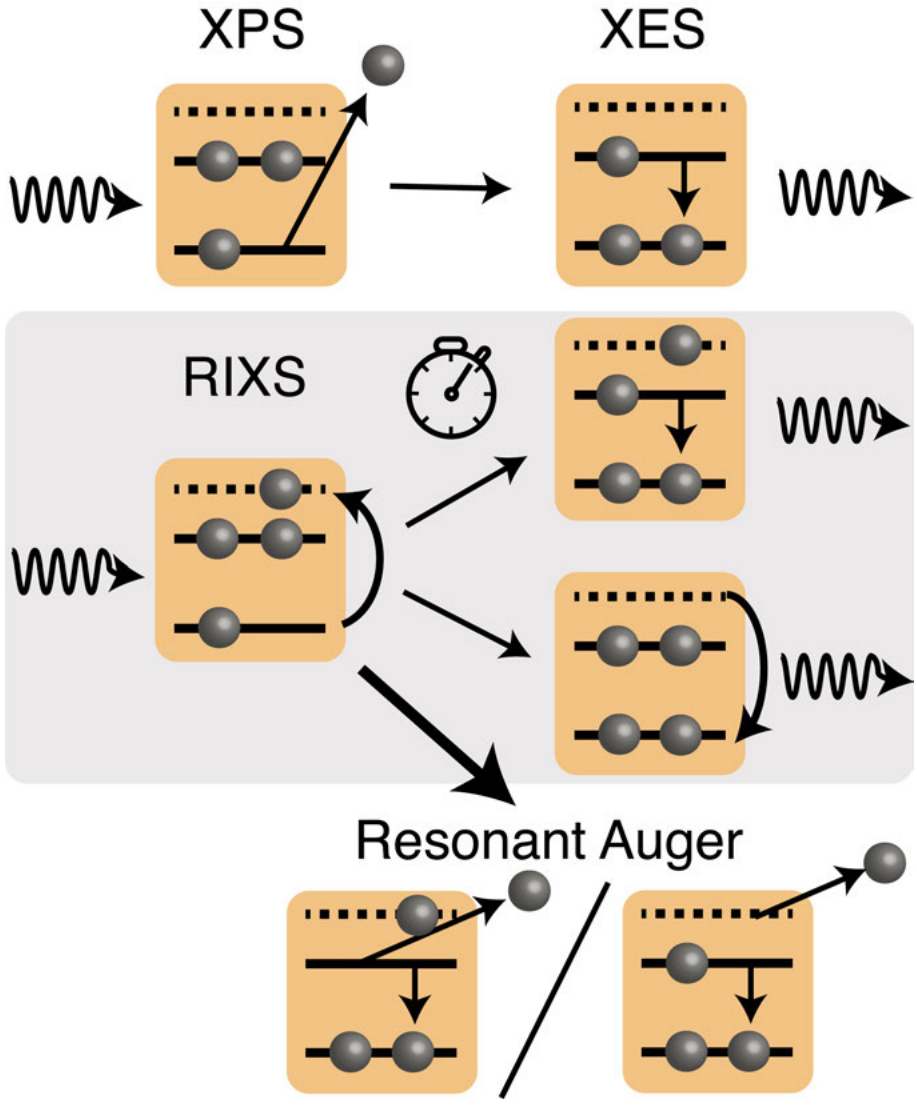

Figure 3.1. Schematic illustration of the photoemission process utilized in XPS, the RIXS process and related techniques.

3.2 Binding energies and what we can learn

Depending on which element and orbital the core electron originated from the BE is different and usually well known. In simple terms, it is the distribution of the nearby charges that will determine the BE. Comparing for example carbon 1s (C 1s) and nitrogen 1s (N 1s) binding energies, it is well known that BE(C 1s)<BE(N 1s). Even if the total charge of atomic carbon and atomic nitrogen is the same, the 1s electron will be more affected by the extra proton in the nucleus of nitrogen than the extra electron due to the geometrical distribution of the wave functions. Such binding energy shifts are, for two elements with similar atomic numbers, on the order of 100 eV.

Apart from identifying elements with XPS, the BE can also give insight of the chemical surrounding. In a molecule, there might be some atoms that attract electrons to a higher degree than others – during the emission process, in such systems, the distribution of electrons can be so different when the electron is emitted for other atoms in the molecule that even the core electrons can have a different binding energy, i.e. chemical shift. These shifts are usually on the order of 1 eV or smaller, which is smaller than the binding energy shifts discussed earlier. For example, one can in ethanol distinguish the C 1s electrons originating from the carbon closest to the hydroxyl group and C 1s electrons originating from the carbon atoms in the alkyl chain.

There are also intermolecular interactions that are strong enough to affect the BE of core electrons. For example in liquids the solvent-solvent or solvent-solute interaction could cause such shifts. In aqueous solutions this is commonly seen for gas-phase and liquid water, both in the valence band and the oxygen 1s. This is usually described as the electron clouds from the surrounding molecules partly screening the nucleus.

3.3 Surface sensitivity and orientation

For a certain kinetic energy ranges XPS can either be considered a surface or bulk sensitive technique. The emitted electrons will first travel through and have a probability of scatter elastically or inelastically against parts of the sample on the way to the detector. One interesting aspect is that the probability of a scattering event, or cross-section, is a function of the KE. The cross-section for inelastic scattering has a maximum at ~100 eV for most materials according to the so called universal curve of inelastic mean free path [35]. At the cross section-maximum the electrons will have the shortest mean free path and the majority of the electrons emitted from the bulk will scatter inelastically before reaching the detector. Though some of the bulk electrons reach the analyzer without energy loss, most of the signal comes from electrons emitted

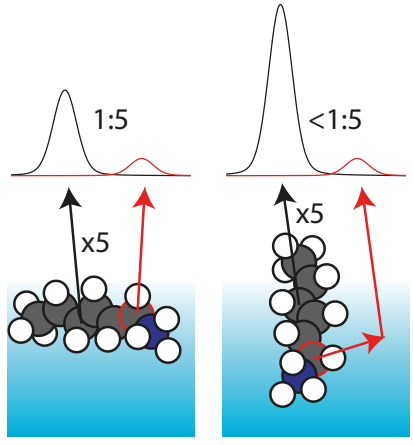

Figure 3.2. In some cases it is possible to deduce the orientation of molecules at the surface. On the right hand side the intensity-ratio is smaller than the stoichiometric ratio, since the electrons emitted from the carbon atom marked with a red ring have a lower probability to escape the liquid.

from the surface. The intensity can be described by:

$$I = k \int_0^\infty \rho(z) \cdot e^{-z/\lambda} dz \tag{3.2}$$

, where k is a constant factor containing photon flux, crossections etc, ρ is the density of the probed atom, λ is the inelastic mean free path and z is the distance perpendicular from the surface which is integrated from the surface to the infinitely deep bulk.

The attenuation effect is even large enough to detect intensity changes on the order of a molecule length. In other words, it is in some cases possible to distinguish if a molecule has a preferred or random orientation relative to the surface.

One example where it is possible to detect such differences is aqueous hexylammonium (a system known to readers of paper II, III and VI). In Figure 3.2, an illustration of two different orientations and the corresponding fabricated spectra is shown. In case of random orientation or where the organic ions are laying flat on the surface (left), the spectral component from the alkyl carbons (with black rings) and the chemically inequivalent carbon (red ring) are weighted the same, i.e. the intensity ratio is close to the stoichiometric ratio. On the right hand side where the organic ion is standing up, the intensity contribution from the alkyl carbons will be higher than the chemically inequivalent carbon. When speaking of orientation, the molecules are not considered frozen or rigid but rather to have a preferred position in which they wiggle around.

3.4 Normalized intensity and stability over time

The actual count number given by the analyzer depends of a multitude of factors like: synchrotron ring current, monochromator slit, overlap between the X-rays and the liquid jet, alignment of the entrance cone to the analyzer (skimmer), voltages that controls the acceptance angles of the spectrometer and other various parameters. Some of these factors will not vary significantly over time during a experiment though others might.

Most of the papers in this thesis compares absolute signals normalized to the acquisition time and the photon flux, something I call normalized signal. Under the assumption that the experimental conditions are stable over time one can translate measured differences in normalized signal between two samples, acquired in proximity (time wise) to each other, as a measure of differences in surface abundance weighted with the exponential attenuation. To ensure that the experimental conditions are stable over time, the valence band of water is monitored of the flushing solution (for example a 50 mM NaCl solution) both prior, in between and after the samples. If the normalized intensity and binding energy positions of both liquid and gas phase water valence band peaks are similar over time we have considered the experiential conditions to be stable. If stability is not ensured the whole data-set is thrown away and has to measured again – a tedious work if unlucky.

3.5 Two layer model and surface enrichment factors

In some of the papers a surface enrichment factor has been derived and used to describe the difference in concentration between the bulk and the surface. The derivation is based upon a two-layer model, first described by Prisle et. al [5], where the probed volume is divided into two separate regions, surface and bulk. This is certainly a simplification since there is most likely no hard boarder between the two regions but rather a more or less gradual change. The model is used to estimate the intensity contribution from the two regions. This is used to estimate the concentration of the probed substance at the surface and use that to calculate the surface enrichment.

The intensity contribution is described as:

$$I_{total} = I_{surface} + I_{bulk} \tag{3.3}$$

. To estimate the bulk contribution a reference sample, often 0.5 M sodium formate solution when C 1s is the edge at interest, is measured. The formate ion ($HCOO^-$) is considered an ion almost exclusively residing in the bulk, which intensity can be approximated by:

$$I_{total}^{formate} \approx I_{bulk}^{formate} \tag{3.4}$$

. Since the intensity per carbon atom in the bulk is considered the same for different samples, the bulk contribution from another solute (in another sample)

can be estimated by:

$$I_{bulk} \approx \frac{c_{bulk}}{c_{bulk}^{formate}} \cdot I_{bulk}^{formate} \tag{3.5}$$

, where c_{bulk} is the bulk concentration of the solute of interest. Even if we now can calculate the surface intensity contribution, the surface concentration is still unknown since the electrons can scatter inelastically. By introducing a sensitivity factor, n, for the two regions, the surface concentration can be estimated. The ratio of the two sensitivity factors, $n_{surface}/n_{bulk}$ is then a measure of relative differences in attenuation based upon the differences in the amount of sample the electrons have to travel through to reach the detector. The ratio have been estimated to be about $n_{surface}/n_{bulk} \approx 0.50 \pm 0.25$ [5]. The intensity ratio between the surface and the bulk could then be expressed by:

$$\frac{I_{surface}}{I_{bulk}} = \frac{k \cdot n_{surface} \cdot c_{surface}}{k \cdot n_{bulk} \cdot c_{bulk}} \tag{3.6}$$

, where k is a constant factor containing experimental conditions like cross-section, photon flux etc. The surface enrichment factor, g, can now be defined and approximated by:

$$g := \frac{c_{surface}}{c_{bulk}} \approx \frac{I_{surface}}{I_{bulk}} \cdot \frac{n_{bulk}}{n_{surface}} \tag{3.7}$$

.

3.6 Measurements at MAX II

Most of the measurements were preformed at the now decommissioned third generation synchrotron MAX II at MAX-lab (or MAX IV as it was called during the last years) located in Lund, Sweden. The papers in this thesis have been based upon measurements mostly preformed at the beamline I411, but also at I1011 with a smaller spectrometer. The principle and specifications were similar for both beamlines. Both beamlines and the setup have been described in the papers and references therein and this will only be a brief description of the setup at the I411 beamline.

I411 was a undulator beamline with a modified SX700 monochromator designed to deliver photon energies of about 50 to 1500 eV [36, 37]. During the later years, it was, for our purposes, not practical to measure at photon energies above 600 eV due to the lack of photon flux. The energy resolution of the X-rays was set by the grating and exit slit – and was chosen to optimize the trade-off with the flux. At the same time, the spectrometer-resolution, set by the pass energy and spectrometer slit, was chosen to match such that no precious photons were wasted. The spectrometer, a SES R4000, was mounted

perpendicular to the X-ray beam on a rotatable chamber such that it was possible to choose which angle of the emission plane that was going to be measured. In our case the "Magic angle" 54.7° was chosen to minimize angular emission effects [38, 33]. The I411 end-station handled both solids at ultra high vacuum (UHV) conditions, but also volatile samples like clusters, gases and liquids. The liquid was introduced through glass nozzle with a inner diameter of about 20 μm, pumped by a HPLC pump though PEEK tubings. The chamber in which the liquid was introduced was a chamber inside the main chamber with a pinhole to introduce the X-rays and a skimmer to the spectrometer for letting the electrons escape. The nozzle was mounted such that it was perpendicular both to the X-ray beam and the spectrometer. The sample chamber was pumped by two large turbo pumps along with a liquid nitrogen coold trap for freezing out the sample. The with flowrates of 0.5 mL/min and with a nozzle size of 20 μm, the speed of the liquid was about 30 m/s. For such speeds, the laminar part of the jet is a few millimeters. The liquid jet was illuminated in the laminar legion and the interaction region was positioned close to the skimmer centered over the acceptance cone of the spectrometer.

4. A few words about RIXS

Resonant Inelastic X-ray Scattering (RIXS) is primarily a bulk-sensitive technique used for characterizing the electronic structure and different electronic and nuclear dynamical properties of solids, gases and liquids. The technique has risen in popularity over the years, especially with the newer and better light sources as the technique is inherently photon hungry in the soft X-ray regime. Since the technique has been described in detail before [39, 40, 41, 42], and RIXS is only a minor part of this thesis, the below description will be quite brief. In order to describe the rather complicated technique, this chapter will first present a simplified description that can help get an intuitive picture. A schematic illustration can be seen in Figure 3.1.

4.1 Two(three?)-step model

Similar to XPS, RIXS uses X-rays to interact with matter. In the simple three-step model the RIXS process can be viewed as; 1) absorption of a photon with energy matching the energy required to create a core hole and exciting the corresponding electron to a bound orbital (called the absorption step). In other words, this increases the energy of the system into an intermediary electronically excited (non ionized) state. 2) During the life time of this intermediary state, the equilibrium positions of the atoms can be perturbed as the result of the new electron configuration. 3) The core hole could now either be filled by the original electron that got excited or another electron in the system, in this de-excitation process a new photon is emitted (called the emission step). The energy of the emitted photon is then slightly lower and the reduction in photon energy carries information about the possible excitations, e.g. electronic and vibrational, of the sample. There is actually another decay channel that is more probable for light elements namely, that instead of step 3) an electron is emitted during the decay (resonant Auger) - this is one of the reasons why RIXS is photon hungry. The adsorption and emission steps are not coupled in this model, which leads to some problems. One problem is interference phenomena between the intermediate states that cannot be explained in the three-step model. The solution can be found in the one step model.

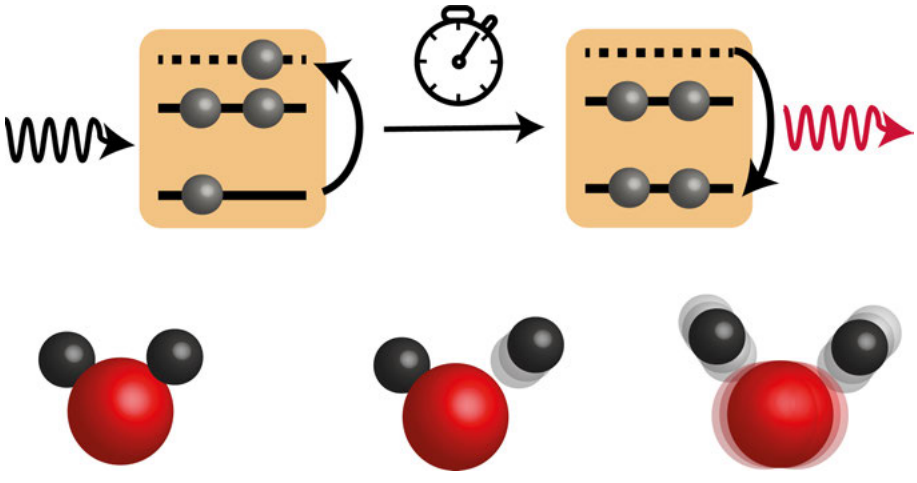

Figure 4.1. Three-step model; by exciting the H_2O O 1s electron on resonance, some of the energy can be transfered into nuclear motion during the life time of the intermediate state before the system returns to its electronic ground state, resulting in vibrations. Note that is only one of the possible final states.

4.2 One-step model

The excitation-emission process can be regarded as a single scattering event, in which the incoming photon transfers a part of its energy to the system, the photon energy loss thus corresponds to an excitation of the sample. This is often via resonant excitation of an intermediate core-hole state, in which the the transition probability of going from the initial state of the system,$|\Psi_0\rangle$,to the final states,$\langle\Psi_f|$, is described by a simplified Kramers-Heisenberg formula:

$$I_f \propto \left| \sum_n \frac{\langle\Psi_f|\hat{p}\cdot\vec{e}'|\Psi_n\rangle\langle\Psi_n|\hat{p}\cdot\vec{e}|\Psi_0\rangle}{h\nu-(E_n-E_0)+i\cdot\Gamma_n/2} \right|^2 \delta(h\nu+E_0-E_f-h\nu') \qquad (4.1)$$

, where $|\Psi_n\rangle\langle\Psi_n|$ are the intermediate states, $\hat{p}$ is the dipole operator, $\vec{e}$ and $\vec{e}'$ are the polarization vectors of the incoming and outgoing photons with energies $h\nu$ and $h\nu'$, E_0, E_n and E_f denote the energy of the initial, intermediate and final states and Γ_n is the intrinsic linewidth of the intermediate state.

4.3 Detuning and vibrations

By changing the energy of the incoming photon slightly below (or above) the resonance energy, i.e. slightly lower (or higher) than energy than required to excite the core electron to the first unoccupied orbital, the scattering duration time, or effective core hole life time will be shorter compared to when at resonance as the total time of the RIXS process can, in time dependent picture, be

described by:

$$T = \frac{1}{\sqrt{\Gamma_n^2 + (h\nu - (E_n - E_0))^2}} \tag{4.2}$$

[42]. This can be used to study nuclear motion (in some systems) during the RIXS process, by correlating the energy losses to vibrational excitations. In the three-step picture the nuclear motion can happen during the life time of the intermediate state, due to the new electron configuration leading to vibrations, illustrated in Figure 4.1.

4.4 Dipole approximation, selection rules and polarization

As already utilized in Equation 4.1, the operator describing the transition from the initial to the intermediate state can be approximated by $\hat{p} \cdot \vec{e}$, for situations when the wavelength of the light is longer than atomic dimensions. The dipole approximation, leads to a set of selection rules the governs what empty orbitals that are possible to excite into. The Δl= $\pm$1 rule limiting the change of the orbital angular momentum by 1 of electrons in atoms (s$\rightarrow$p,p$\rightarrow$s,p$\rightarrow$d etc) is similar for molecular orbitals ($\sigma \rightarrow \pi$,$\pi \rightarrow \sigma$) in systems with certain symmetries. For linear polarized light there are also rules for $\sigma \rightarrow \pi$ transitions that constrains the empty valence orbital to be spatially parallel with the polarization vector (or at least not perpendicular to the polarization vector). For a fixed orientation of a molecule the absorption cross section of horizontally and vertically polarized light can be very different on resonance. This could also affect the emission step depending on the symmetry of the occupied molecular orbitals that potentially could fill the core hole. This could result in an anisotropy even for gas phase molecules with random orientation.[43, 39]

5. Summary of papers

Largely, this thesis is based upon papers probing different types av solute-solute and solute-solvent interactions that contributes to a change in the equilibrium between surface and bulk. Partly this is specifically about ion-ion interactions in aqueous solution, in this case, contact ion pairing (paper I and II). To my knowledge, this is the first time ion pairs have been observed with XPS, though attempts has been made. In paper I we see indirect evidence of ion pairing and in paper II we can report a binding energy shift originating from ion pairing on the aqueous-vacuum interface.

In the second part, paper III-V, surface enrichment due to van der Waals interactions and water competition of organic compounds are studied and analyzed with a Langmuir isotherm adsorption model.

Paper VI investigates how the acid and base fractions for organic acid and bases changes at the aqueous surface as a function of bulk pH – addressing the question whether the pH or pK_a values are different at the surface.

Paper VII contains preliminary results of aqueous carbonate and bicarbonate solutions probed with RIXS.

5.1 Ion pairing and surface effects (Paper I and II)

Papers I and II are motived from molecular biology (paper I) and atmospheric science (paper II) – systems which contain a lot of water. Real systems are rather complex to understand on a molecular level but can be modeled by more simple aqueous solutions. In order to figure out how multicomponent systems work one can, depending on the system, either try out various combinations of the the single components or use some kind of model system. It is for example useful to study a smaller but somewhat similar system instead of a whole protein since a system with many atoms tend to be rather difficult to analyze with spectroscopy. Atmospheric droplets usually contain a multitude of compounds and the problem there is to disentangle the direct and indirect interactions between the solutes.

In certain systems the interface between an aqueous solution and a hydrophobic environment like air or fatty parts of a protein can be of interest. Such interfaces can be modeled by a water/vacuum interface instead, so that it possible to probe the model system with the surface and chemically sensitive XPS technique. In papers I and II MD simulations and XPS have been used

to study surfaces of aqueous solutions containing ions. Specifically, these systems are aqueous solutions with two salts which are compared to solutions with only one of these salts. To probe surface abundance XPS normalized intensities have been compared – see Section 3.4 for details regarding normalized intensities. By comparing the surface abundance between the single and mixed solute solutions one can learn something about the relationship between the solute-solute interaction and the surface-bulk equilibrium.

There are a number of factors that can affect the surface propensity of a molecule/ion. Generally, the higher charge an ion has, the stronger hydrated it is which hence reduces the surface propensity as the ions gain hydration energy from the surrounding water molecules. On the other hand the more/-longer alkyl chains a species has, the more hydrophobic and more surface enriched the species is. Indirect mechanisms can also be important, where other species in the same solution competes for water to stay hydrated and push the other species out to the surface. There are also more intricate mechanisms, like cooperative surface enrichment which will be discussed for paper II.

5.1.1 Salting in or salting out? (Paper I)

The guanidinum chloride salt, $C(NH_2)_3Cl$ (GdmCl) and disodium sulphate salt, Na_2SO_4 are the protagonists in paper I. The guanidium cation (Gdm^+) is, in biochemistry, used as a strong denaturant agent for proteins but have been seen to instead stabilize proteins when SO_4^{2-} ions are present [44, 45]. Though the reason is debated, ion pairing between Gdm^+ and SO_4^{2-} was suggested among other explanations. By comparing the N 1s normalized intensity of a solution with only GdmCl to a solution with GdmCl + Na2SO4 or GdmCl + NaCl the abundance of Gdm^+ ions at the surface could be directly compared between the three solutions as the bulk concentration of Gdm^+ was the same. As interpreted from the intensities in Figure 5.1(a), there are more Gdm^+ ions at the surface in the solution with NaCl than in the "pure" GdmCl solution which in turn has more than the solution with Na_2SO_4. To start with the simple case, in comparison to the "pure" GdmCl solution the Gdm^+ ions are "salted out", i.e. pushed to the surface by the additional Na^+ and Cl^- ions in the solution with NaCl. The Na^+ and Cl^- ions are most likely more strongly hydrated than the Gdm^+ ions and with the lack of water molecules to properly hydrate Gdm^+, the Gdm^+ ions are pushed to the surface. This is also confirmed by the MD density profiles in Figure 5.1(c,e), where the black profile (Gdm^+) is higher in the solution with NaCl. Note that some of the Cl^- ions (green) follow the Gdm^+ ions to the surface. Actually, according to the Radial Distribution Function (RDF) from MD, Gdm^+ forms contact ion pairs with Cl^-, as indicated by the ~ 4 Å feature (blue dotted) in Figure 5.1(b).

The more complicated case is the solution with GdmCl + Na_2SO_4, where the the amount of Gdm^+ ions at the surface is reduced compared to the "pure"

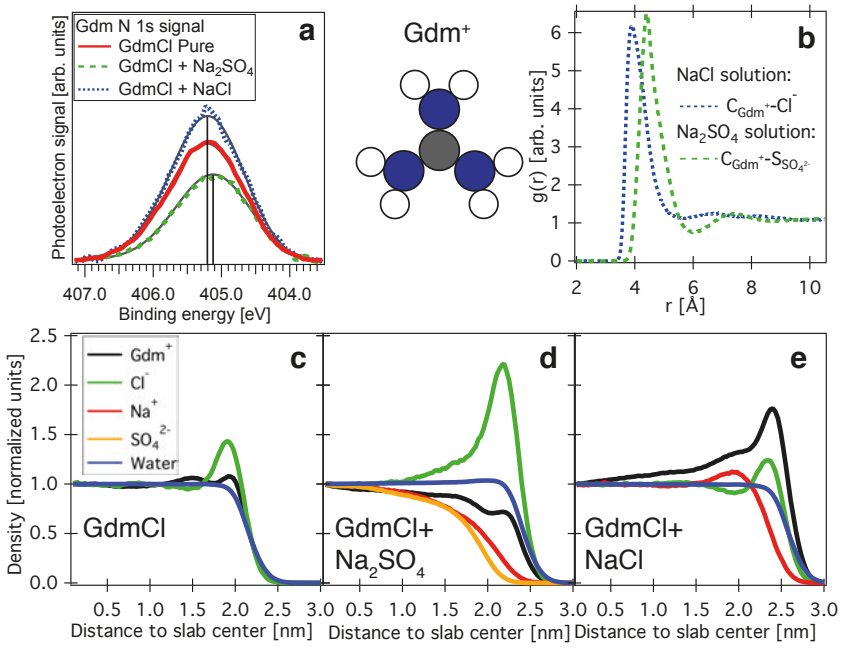

Figure 5.1. The surface concentration of Gdm^+ ions can depending on the other ions in the solution either increase or decrease compared to a solution with only the GdmCl salt.

solution, see Figure5.1(a). This is unexpected since the SO_4^{2-} ion, if anything, is efficient at "salting out" other species since it is, with its double charge, confining a lot of water as hydration shell-water around itself. The sharp peak at about 4.5 Å, C_{Gmd^+}-$S_{SO_4^{2-}}$ RDF (green dashed) in Figure 5.1(b), tells us that Gdm^+ and SO_4^{2-} also forms contact ion pairs. The strong hydration of the SO_4^{2-} ions seems to be enough to "drag" the Gdm^+ ions from the surface even as an ion pair.

Though this is a special case, it shows that the surface propensity of solutes do not necessarily have to increase if salt is added to an aqueous solution. It would be interesting to see if and at what concentration of added Na_2SO_4 the Gdm^+ would be "salted out" instead.

5.1.2 What happens at the surface when mixing two organic ions together? (Paper II)

Paper II investigates a quite different system compared to paper I. Here the interaction between two atmospherically relevant compounds, hexylammonium chloride ($CH_3(CH_2)_5NH_3Cl$; $HexNH_3Cl$) and sodium hexanoate ($CH_3(CH_2)_4COONa$; NaHexOO) are examined. Initially this system was believed to have a chance of donating a proton from hexylammonium to hexanoate at the surface, inspired by earlier work [5, 46] – though this was not the case, other interesting surface effects were seen.

In solution with a pH value of 7 hexanoate ($CH_3(CH_2)_4COO^-$,$HexOO^-$) will be the predominant protonation form since the pK_a value of hexanoic acid is 4.88 [47]. To my knowledge there have only been reports of acidic aerosols containing hexanoic acid but no neutral or alkaline aerosols containing hexanoate. Similarly, there have been reports of aerosols containing hexylamine (the deprotonated form of hexylammonium) [48] in alcalic aerosols but no hexylammonium in neutral or acetic ones. Since the pK_a value of hexylammonium is 10.56 [49], hexylammonium would be the dominant protonation at a pH value of 7. Simplistically there should at least be a chance of both hexylammonium and hexanoate coexisting in an atmospheric droplet at the same time if the pH value would be somewhere in between the the two pK_a values roughly at pH 7.7.

One characteristic thing about both organic ions is that they are both hydrophobic and hydrophilic, i.e. amphiphilic. The functional groups are charged and more or less hydrophilic, while the alkyl chains, with the lack of ability to form hydrogen bonds, are hydrophobic.

C 1s and N 1s XPS normalized intensities are compared, while the interpretation is a tad more complicated than in paper I. Since the organic ions are elongated, the orientation of the organic ions relative to the surface can affect the normalized intensity from the different atomic sites, see Section 3.3 for a specific discussion about the surface sensitivity of XPS and orientation.

The C 1s spectra of the single solute solutions are shown in Figure 5.2(a); 100mM $HexNH_3Cl$ (blue dashed-dotted), 100mM NaHexOO (red dashed-double-dotted). Both species are surface enriched at these concentrations, as was confirmed by both MD and normalized intensity comparisons to a 500 mM sodium formate solution measured in direct succession. By calculating the intensity ratios of the two spectral components in the two single solute solutions, C_C/C_N and C_C/C_{OO}, the orientation of the organic ions relative to the surface can be estimated. The $HexNH_3^+$ ions seem to have random or flat orientation while the intensity ratio of $HexOO^-$ ions imply that they are orientated such that the alkyl chains are pointing out of the surface towards the vacuum. A detailed discussion of the orientation of the organic ions according to MD can be be found in the SI of Paper II.

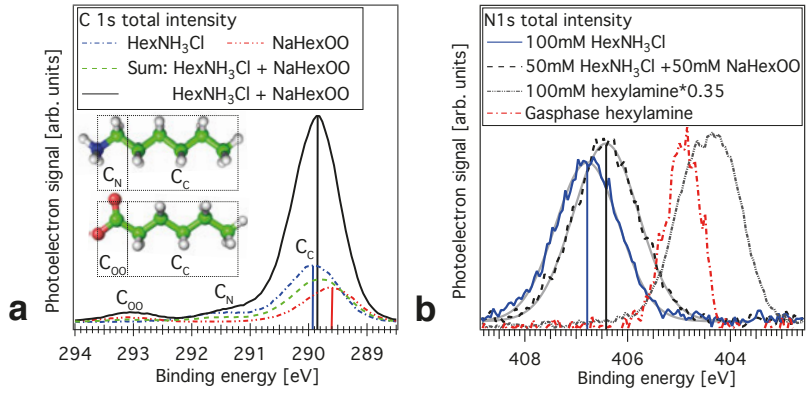

Figure 5.2. N 1s spectra of Hexylamine ($HexNH_2$), the neutral form of $HexNH_3^+$, were also recorded for both gas phase and liquid phase to verify that the proton was not transfered in the mixed solute solution.

Continuing with the mixed solute system, in Figure 5.2(a), an artificial sum of the spectra from the single solute solutions (green dashed) is presented along with the spectrum of the real mixed solute solution (black solid), 50mM $HexNH_3Cl$ + 50mM NaHexOO. By comparing the total intensity of the artificial sum (which is divided by 2 to compensate for concentrational differences) and the real mixed solute solution, it is clear that one or both of the organic ions are even more surface enriched than in the single solute solutions. This can also be seen in Figure 5.2(b), where the N 1s spectra of the single and mixed solute solutions are shown. The intensity of the N 1s peak in the mixed solute solution is slightly more intense even though the concentration is half compared to the single solute solution. As pointed out previously, orientational changes affect the different spectral components differently and when the surface enrichment happens at the same time, total intensities are even trickier to interpret. The increased C_C intensity could be explained by the alkyl chains pointing out of the surface and since C_N and N 1s also increases this speaks for an even stronger surface enrichment of the $HexNH_3^+$ as these peaks otherwise would decrease in intensity with this orientation. After careful analysis of the C 1s spectra, it seems like the most significant change between the single and mixed solute solutions are the $HexNH_3^+$ ions undergoing a re-orientation along with an increased surface enrichment, though the $HexOO^-$ are also probably more surface enriched.

An illustration of the surface enrichments and the orientation in the different solutions are shown in Figure 5.3. The N 1s spectra in Figure 5.2(b) also displays an interesting binding energy shift between the single and mixed solute $HexNH_4Cl$ solutions. The binding energy shift of 0.36 eV is rather large and the direction towards lower binding energy indicates the presence of a negative charge in proximity to the headgroup. The binding energy shift is

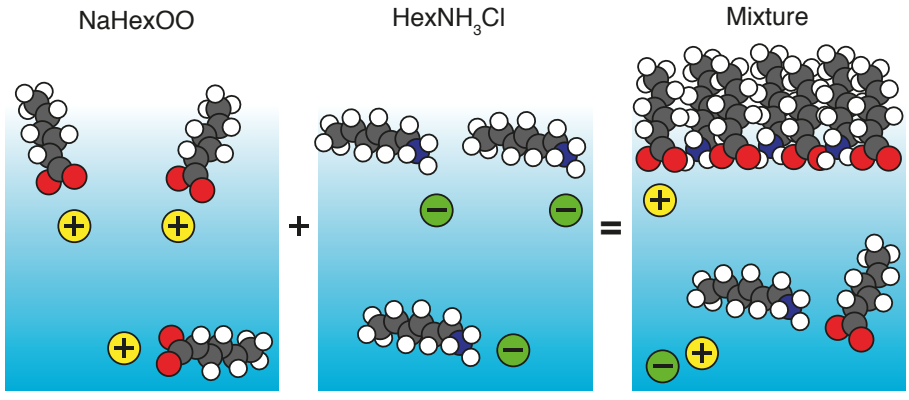

Figure 5.3. Schematic illustration of how the orientation and surface enrichment are believed to change, comparing the single solute solutions with the mixed solute solution.

interpreted as ion pairing between the two organic ions as ion pairing was also confirmed by the RDF from MD, Figure 5.4. A distance between the nitrogen in $HexNH_3^+$ and the two oxygens in $HexOO^-$ of 2.8 Å (the closest oxygen in $HexOO^+$) to 4-5 Å (the second oxygen in $HexOO^+$) classifies this as a contact ion pair.

However, as shown in the two MD snap shots in Figure 5.5 the organic ions are not forming binary pairs but gather in larger clusters at the surface. To understand the structure of the clusters better several RDF were calculated and are presented in Figure 5.6(a,b) along with a calculation of the distance between two organic ion of the same kind versus the angle formed with a organic of opposite charge (c,d).[1] Without going into too many details, the clusters in the mixed solute solution resembles zig-zag chain like structures with organic ions of alternating charge. From the histograms the angles, as defined in Figure 5.6(c,d), are determined to α=99°±4°, β_A=76°±4° and β_B=130°±10°. Region A, in Figure 5.6(b,d), is believed to correspond to a structure with two $HexNH_3^+$ ions per $HexOO^-$ and region B to three $HexNH_3^+$ ions per $HexOO^-$.

The clustering can be explained by ion pairing between the headgroups of the organic ions, van der Waals interactions between the alkyl chains and the lack of water molecules around the alkyl chains. At the same time, the organic ions are even more surface enriched compared to the single solute solutions. Since the clustering is facilitated by increased surface enrichment and the surface enrichment is facilitated by the clustering this mechanism is called a cooperative effect. This could be of relevance to atmospheric droplets since this and similar systems (organic compounds with opposite charge) could already at very low bulk concentrations be very surface enriched.

[1] A pseudo code for filtering and calculating the angle versus distance plot is shown in Listing 5.1.

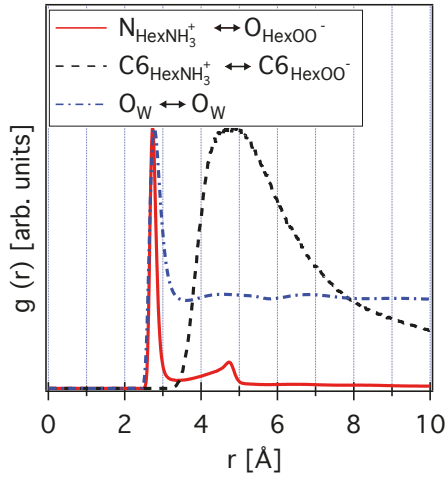

Figure 5.4. According to the MD simulations the organic ions form contact ion pair between the headgroups while the alkyl chains dangles back and forth at larger distances.

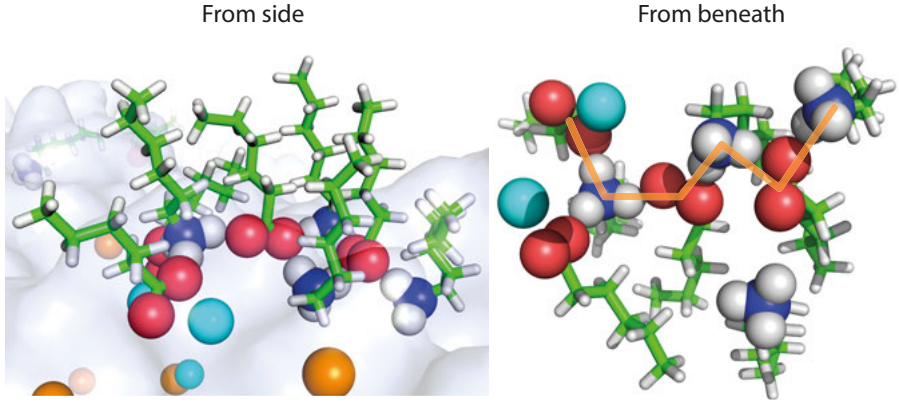

Figure 5.5. Same cluster from two different point of views. The orange line is an example of how the zig-zag chain could look like.

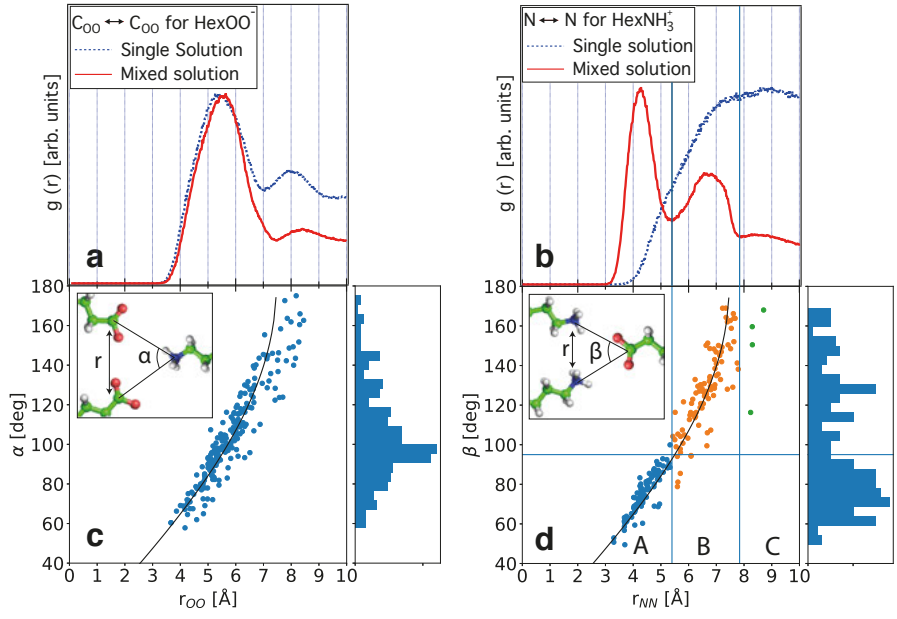

Figure 5.6. Panel (c) and (d) are only displaying correlations for the mixed solution, and is why they should only be compared to the red solid lines in panel (a) and (b). (c,d) the black line represents the circle segment of a circle with a radius of 3.73 Å – the mean distance between $N_{HexNH_3^+} \leftrightarrow O_{HexOO^-}$ given by the RDF in Figure 5.4.

Listing 5.1. Psuedo code for filtering triplets and calculating angle vs distance.

```
#Species A could be all carboxylate-carbons of hexanoate and B
    could be the nitrogen atoms of hexylammonium.
Load MD trajectories.

Indexation of position vectors of members of species A & B.

#Angle vs distance will only be calculated for distances smaller
    than Threshold between members in A and B.
Threshold = reasonable value #5 Åin Paper II.

For all time steps
   For all pairs in A #A1,A2 in each pair
      For all members in B
         If (distance(A1<->member in B)<Threshold and
              distance(A2<->member in B)<Threshold)
            Calculate & save the angle formed by A1-B-A2 & the
                distance between A1 & A2.
```

5.2 Langmuir adsorption (Paper III-V)

As described earlier organic compounds are interesting for atmospheric reasons since they can accumulate in large quantities at the surface of cloud droplets and affect water accommodation and evaporation. Most of the results in the following sections are supported by MD-simulations, though the summary will be focused on the experimental results.

5.2.1 Surface abundance

In paper III-V the abundance and orientation of different amphiphilic organic compounds at the aqueous surface have been probed with XPS while changing the bulk concentration. In all three papers, the XPS signal (i.e. measure of surface abundance) of the organic compounds increases with increasing bulk concentration, but quite non-linearly as the surface signal gradually saturates. A typical C 1s spectrum for these systems can be seen in Figure 5.7, where the two spectral components represent two inequivalent carbon types, the alkyl chain carbons (C_C) and the alpha carbon (C_α). The sum of the total intensities is used as a measure of the surface abundance. The saturation process was similar for alkyl carboxylates, alkyl ammonium (paper III) and linear and non-linear alcohols (paper IV-V). In Figure 5.8(a) an example from paper IV can be seen, here the C 1s total intensity of 1-pentanol and 3-pentanol is compared as a function of bulk concentration. Even if the surface saturation process looks similar for all systems within the papers, the rate of change and the absolute intensities were different as can also be seen in the figure. To analyze the saturation process and the surface-bulk equilibrium for the solutes, a Langmuir isotherm adsorption model have been applied, described in Section 2.2. One of the more interesting assumptions is that the difference of Gibb's free energy of surface adsorption, ΔG_{Ads}, for a solute in the bulk compared to the surface is constant and independent of the bulk/surface concentration. As mentioned, the assumption is probably poorly fulfilled when the surface is close to saturation since the solutes are close enough to interact. In some cases, two slightly different ΔG_{Ads} values are given depending if one fits the Langmuir model with more weight at lower surface saturations or the region with higher surface saturation. The model with a single ΔG_{Ads} have worked reasonably well and can to the first approximation give some insight to the surface-bulk equilibrium.

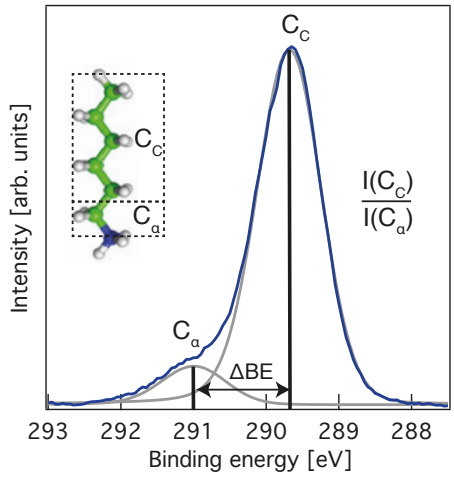

Figure 5.7. Visual example of how the ΔBE and the intensity ratio is calculated. The spectrum is C 1s spectrum of 600 mM $HexNH_3Cl$ at 360 eV photon energy.

5.2.2 Orientation

As explained in Section 3.3, the intensity ratio C_C/C_α can give insight to the compound's orientation. Due to electron attenuation over distances on the order of molecular dimensions, electrons from a slightly deeper region will scatter inelastically with a higher probability than electrons emitted from a region closer to the vacuum. Hence, a higher ratio than the stoichiometric ratio is possible and indicates that the compound has a non-random orientation at the surface. For some of the compounds in paper III-V the intensity ratio changes significantly with concentration. A plot with the intensity ratios for the alcohols can be seen in Figure 5.8(b). With increasing concentration the deviation, i.e. reorientation effect, increases. Hence, the alkyl chains points more outward from the surface as the bulk concentration increases. Interestingly, the effect is larger for compounds with longer alkyl chains and occurs at lower bulk concentrations. The reorientation seems to level out in the same region as the surface is saturated, which indicates that it is the interaction between the solutes that drives the reorientation. As the surface gets more crowded, the organic compounds are believed to reorient themselves to form a more compact structure which allows for a higher surface concentration, still resembling a monolayer. The same effect, but smaller, is also seen for the non-linear alcohols. In that case of 3-pentanol the two alkyl chains are believed to both bend towards the surface.

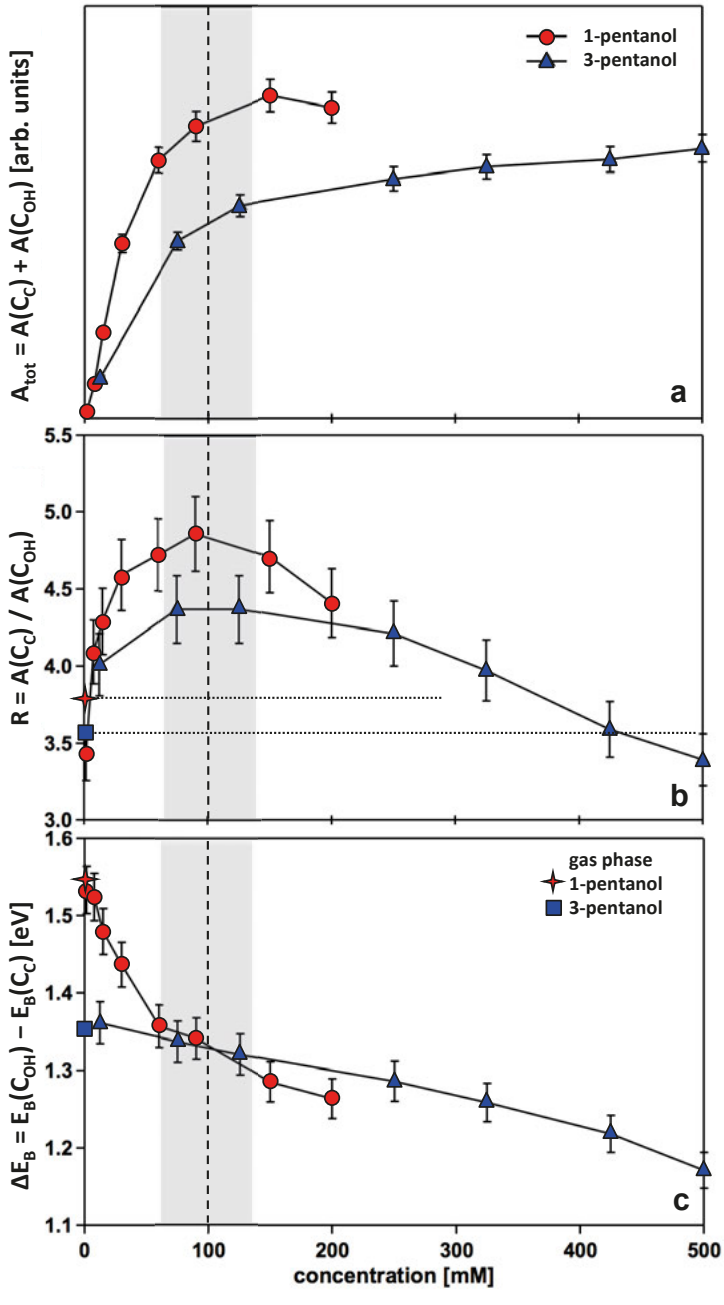

Figure 5.8. Note that the intensity ratio R in (b) and the binding energy difference ΔBE in (c) for 1-pentanol drastically change from the low surface signal until a monolayer is believed to be formed (the dashed line in (a)).

5.2.3 Dehydration and binding energy shifts

A simultaneous change in the binding energy difference between the two spectral components, ΔBE = BE(C_α)-BE(C_C), is also observed as the molecules change their orientation. An example for 1-pentanol is shown in Figure 5.8(c), where the distance between the two peaks shrinks from about 1.55 eV to 1.27 eV over the range 0-200 mM. Similar shifts in the binding energy splitting is also observed for the other systems – though not as pronounced for the non-linear and shorter compounds. As the alkyl chains gradually stand up due to the higher surface concentration of the organic compounds, they become less hydrated. Instead of hydrogen bonding with the surrounding water the alkyl chains are believed to instead bond via van der Waals interaction. The change in ΔBE, for 1-pentanol, is mostly originating from a change in the binding energy of the C_C peak, which supports this idea. Since the water molecules have a dipole moment, they can partly screen the atomic nucleus and thus lower the binding energy of the electrons. This is the same reason for why gas phase spectra, if not always, at least in most cases has a higher BE compared to liquid phase spectra of the same compound. The BE shift should be similar for all core electrons going from gas phase to a fully solvated compound. In Figure 5.8(c) the BE splitting between the two peaks for gas phase is also shown – a value similar to the corresponding shift for the lowest bulk concentration. The change in the BE splitting hence support the idea of the alkyl chains no longer are fully hydrated, as the change in ΔBE has to originate from a non homogeneous hydration.

5.2.4 An attempt to formulate a building block model for surface adsorption

ΔG_{Ads} values are given by fitting the Langmuir isotherm model to the surface signal-data. As previously explained, ΔG_{Ads} is the difference in Gibb's free energy between a solute in the bulk compared to the surface. The more negative this value is the more energy is gained for a solute if migrating to the surface. This value is, for the linear alcohols, more negative the longer the alkyl chains are. In other words, the more hydrophobic a compound is the more likely it is to be found at the surface. A compilation of ΔG_{Ads} values from different papers regarding amphiphilic compounds are displayed in Figure 5.9. For the linear alcohols ΔG_{Ads} seems to change linearly with the number of carbons in the compound, from linear fitting about -2.3±0.50 kJ/mol/carbon. This means that the "amount of hydrophobicity" changes linearly with the number of carbons – which seems reasonable. Though the number of points are really too few to claim something general with certainty, it seems that ΔG_{Ads} per carbon is similar for other compounds with other head groups as well as the non-linear alcohols. If the adsorption mechanism would be similar for other headgroups, a similar change in ΔG_{Ads} per carbon would also be

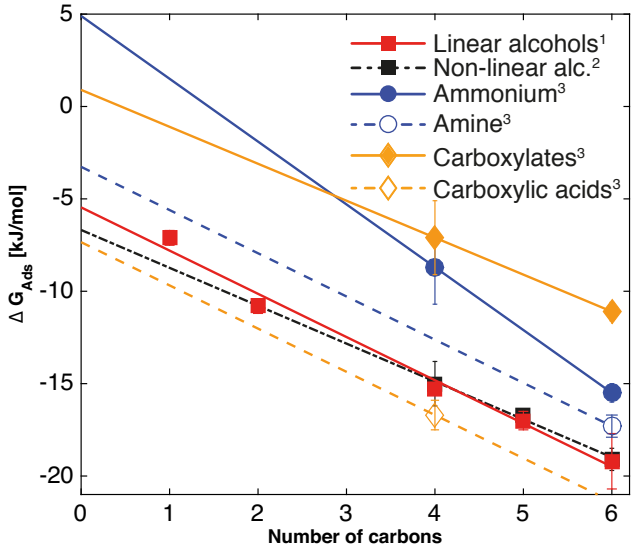

Figure 5.9. Collection of ΔG_{Ads} values from several papers and fitted/predicted ΔG_{Ads} for other alkyl chain lengths. The dashed lines have the exact same slope as the fitted one from the linear alcohols to illustrate how the building block principle could be used. ΔG_{Ads} values from 1: Ref [50, 31, 51], 2: Ref [31], 3: Ref paper VI.

reasonable to expect. As a first approximation one could use the ΔG_{Ads} per carbon from the linear alcohols to calculate the ΔG_{Ads} contribution of the OH group, i.e. where the line intersect 0 carbons. In the best case scenario this could be done for more headgroups help predicting ΔG_{Ads} values for compounds with several headgroups by simply adding the predicted ΔG_{Ads} values. This would certainly require many additional measurements to establish, though if an empirical model would be feasible it could save a tremendous amount of time as these measurements are very time consuming.

5.3 Are the pH and the pK_a values at the surface different compared to the bulk? (Paper VI)

For small droplet and aerosols the pH value can have a large effect on the chemistry but also surface effects as the one seen paper II. One could argue that the pH value is rather easy to measure for the bulk and by titration also finding out the pK_a values for acids. Though it is not as easy to measure for aerosols and even harder to know for interfaces. The equilibrium between the acid and the conjugated base in an aqueous solution is usually described as:

$$H_2O + HA \rightleftharpoons H_3O^+ + A^- \tag{5.1}$$

,where $[HA]$ is the acid concentration and $[A^-]$ is the concentration of the corresponding conjugated base. For weak acids and dilute solution the Henderson-Hasselbalch equation can be used for describing the relationship between pH and pK_a [52];

$$pH = pK_a + log\left(\frac{[A^-]}{[HA]}\right) \tag{5.2}$$

. This relationship can expressed as the acid fraction with some manipulation:

$$F_A = \frac{[HA]}{[A^-]+[HA]} = \frac{1}{10^{(pH-pK_a)}+1} \tag{5.3}$$

. Since many bulk phenomena differ from surface phenomena, it is natural to ask whether the pH value or pK_a values are different at the surface. For some time this has been debated (see references within paper VI), though no consensus seems to have been reached. Even if there are surface effects on pH and pK_a – there seems to be other mechanisms dominating the base/acid speciation at the surface for the studied organic acids/bases. In Figure 5.10(a), the acid fraction at the surface for butyric acid (ButOOH) is shown as a function of bulk pH. The fraction is extracted from XPS, where ButOOH can be distinguished from the conjugated base butyrate ($ButOO^-$). The shape of the data is similar but shifted to the corresponding curve for the bulk (also shown in green). From fitting an apparent pK_a value (pK_d^*) can be found at a higher pH value. It is called apparent pK_a since it is not yet clear weather the pK_a or pH is different or not at the surface. In Figure 5.10(b) from XPS, estimates of surface concentrations of ButOOH, $ButOO^-$ and the sum of both species are shown. The surface concentration of the two forms are clearly different, where the ButOOH is very much more abundant at low pH values compared to $ButOO^-$ at higher pH. In some sense this is not surprising since, as discussed, charged forms in general are stronger hydrated compared to a corresponding neutral compound. Langmuir isotherm adsorption curves were also measured for these compounds – confirming that ΔG_{Ads} was more negative for the charge neutral form. At a given pH the acid fraction at the surface would then be dominated by difference in ΔG_{Ads} values rather than a difference in pH or pK_a at the surface. One can describe this as a net effect of three equilibria as illustrated in Figure 5.10(c), two describing the surface-bulk equilibria of the respective acid/base form with a Gibb's free energy of surface adsorption similar to paper III-V and one describing the normal acid-base bulk equilibrium. By introducing a relative enrichment factor, g, for the conjugated acid/base pair a modified acid fraction model can be made to compensate for the differences in surface abundance between the two species. The enrichment factor a single species is an estimate of the fraction between the surface concentration and the bulk concentration, $g_{HA} = [HA]^s/[HA]$, where $[HA]^s$ is the estimated surface concentration of the acid and $g_{A^-} = [A^-]^s/[A^-]$ for the base-form. By substituting the bulk concentrations by the surface concentration and the surface enrichment factors the Henderson-Hasselbalch equation can be expressed

as:

$$pH = pK_a + log\left(\frac{[A^-]^s}{[HA]^s} \cdot \frac{g_{HA}}{g_{A^-}}\right) \tag{5.4}$$

. The acid fraction for the surface can then be expressed as:

$$F_A^s = \frac{1}{10^{pH-pK_a-log(g_{HA}/g_{A^-})}+1} \tag{5.5}$$

. By now realizing that $log(g_{HA}/g_{A^-})$ will "shift" the acid fraction curve, the apparent pK_a can now be model through the enrichment factors by defining:

$$pK_d^* = pK_a - log(g_{HA}/g_{A^-}) \tag{5.6}$$

From these enrichments factors, the predicted surface acid fraction curve (red solid line) is fairly similar to the measured acid fraction, shown in Figure 5.10(d). Corresponding measurements and analysis where made for hexanoic acid (HexOOH), butylamine ($ButNH_2$) and hexylamine ($HexNH_2$), with similar results. In the case of the amines the base (neutral charge vise) was also promoted compared to the corresponding conjugated acid form (charged) and pK_d^* shifted towards the lower pH values accordingly.
Even if the pH and pK_a values are possibly different at the surface, the different surface propensities resulting from charge versus lack of charge for organic acid/bases seems to be the dominating effect for the acid/base fraction at the surface. By knowing the surface enrichment factors for other compounds one could hopefully predict how the surface composition changes as a function of pH. Hopefully this could be useful for modeling aerosols as the pH values and the surface compositions are difficult to probe.

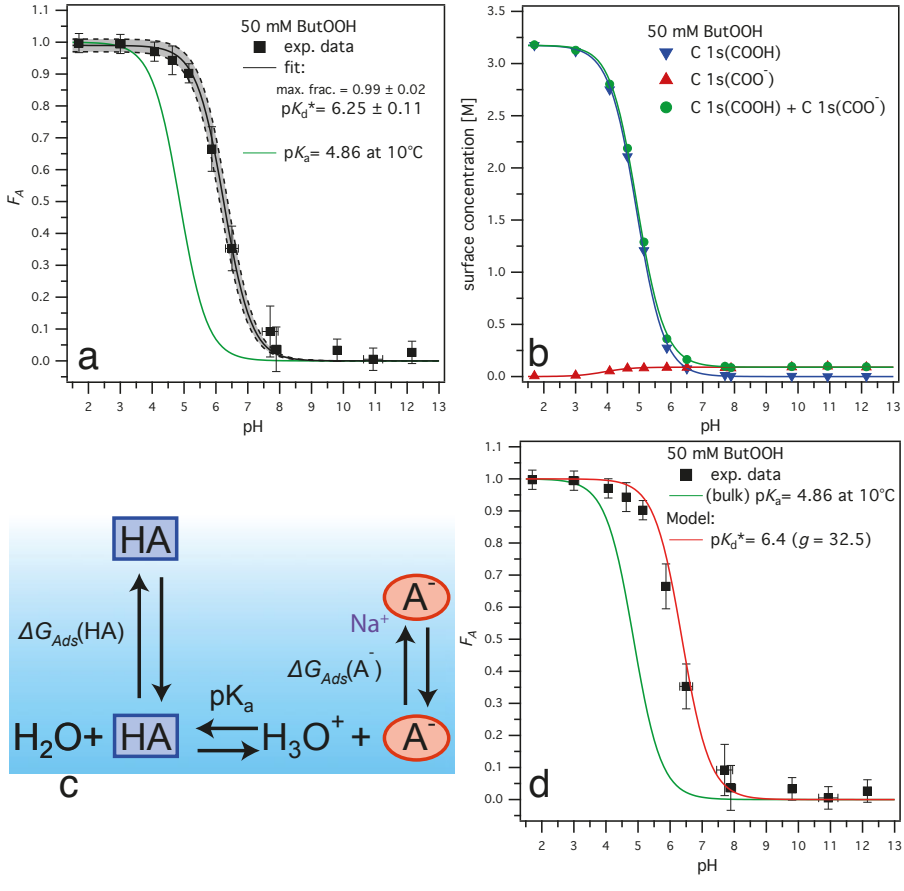

Figure 5.10. (a) Surface acid fraction and (b) estimated surface concentrations for ButOOH and the corresponding conjugated base $ButOO^-$ are shown as well as (d) the predicted surface acid fraction from surface enrichment factors. (c) An illustration of the three equilibria used to model the acid fraction.

5.4 Protonation affecting electronic states of carbonate (Paper VII)

Gaseous carbon dioxide (CO_2) can hydrate in small amounts but in its aqueous phase react with water and form carbonic acid (H_2CO_3). One concern with increasing CO_2 levels in the atmosphere, is that the equilibrium can shift and hence lead to lower pH values for seas and lakes, with potential negative consequences for ecosystems. H_2CO_3 has two other protonation states; bicarbonate (HCO_3^-) and carbonate (CO_3^{2-}). Aqueous solutions of Na_2CO_3 and $NaHCO_3$ are investigated at the O K-edge with RIXS. The CO_3^{2-} ion is trigonal (planar) with D_3h symmetry, while the HCO_3^- is planar but with broken symmetry. The investigated O 1s$\rightarrow \pi^*$ resonance at 533.3 eV, is below the O 1s pre-edge of liquid water situated at 535 eV. This allows partial selective excitation of CO_3^{2-} and HCO_3^-, even though as seen in Figure 5.4, there is still plenty of signal from water at the two excitation energies (532.8 eV, 533.3 eV). An estimation of the water contribution in the spectra of the two solutions has been attempted by subtracting as much as water signal as possible without getting negative values. At a photon energy of 532.8 eV, the excitation is slightly detuned below the resonance which is believed to reduce the scattering duration time [39]. The reduced scattering time can be seen in the vibrational profiles for water by comparing panels (c) and (d) in Figure 5.4. This is also seen for the two ions in Figure 5.4 (a,b) where the energy loss tail of the elastic peak is longer and more intense on resonance than when detuned. The lack of distinct peaks is probably a combination of coupling with the surrounding water molecules and limitations of the spectral resolution. The vibrations of HCO_3^- seem to be more intense compared the vibrations of CO_3^{2-}, which could be associated with the reduced symmetry in HCO_3^-. Note that the lack of clearly visible OH-vibrations (0.46 meV) in HCO_3^- could come from an overestimation of the spectral contribution from water. The assignment and analysis of the electronic states in Figure 5.4(a,c) have been done previously on resonance [53, 54]. The detuning and polarization dependence are unique features in Paper VII. Over only a 0.5 eV wide excitation energy interval the two high energy features are drastically changed.

The high energy peak corresponds to the highest occupied molecular orbital (HOMO) and shape is ,according to calculations [53, 55], similar to a p-orbital with the nodal plane parallel with a line formed by the oxygen and the carbon, for all oxygens including the protonated one.

Nuclear motion and/or selective excitation could explain the dramatic changes, though further analysis is needed. The electronic states are similar for two ions except for the extra feature at 522.5 eV in bicarbonate, which probably is there due to the protonation and perhaps an effect of the broken symmetry. If this would be the case, this could perhaps be used to study symmetry breaking of carbonate ions in solid or amorphous materials. The polarization effect seems to be largest for the HOMO for both ions though strongest

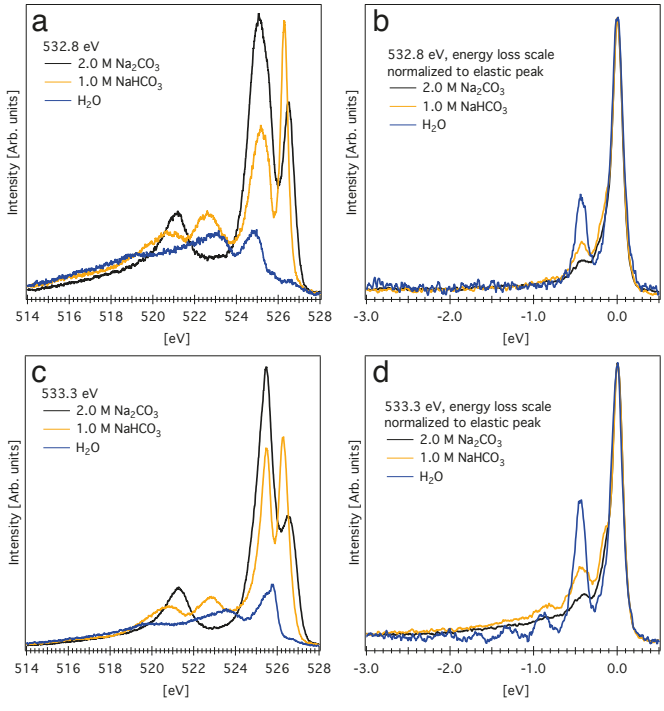

Figure 5.11. The detuning effect is visible for the two samples including pure water.

for HCO_3^-. During the absorption step the O 1s$\rightarrow \pi^*$ transition will favor carbonate ions which molecular plane is perpendicular to the polarization plane. This will in the emission step lead to an anisotropy, probably due to the shape of the HOMO. It is surprising that the polarization effect is stronger in HCO_3^-. It is hard to judge if it is in the absorption or emission step the effect comes from, hence one has to take a closer look at the shape of HOMO and LUMO on the different oxygen sites.

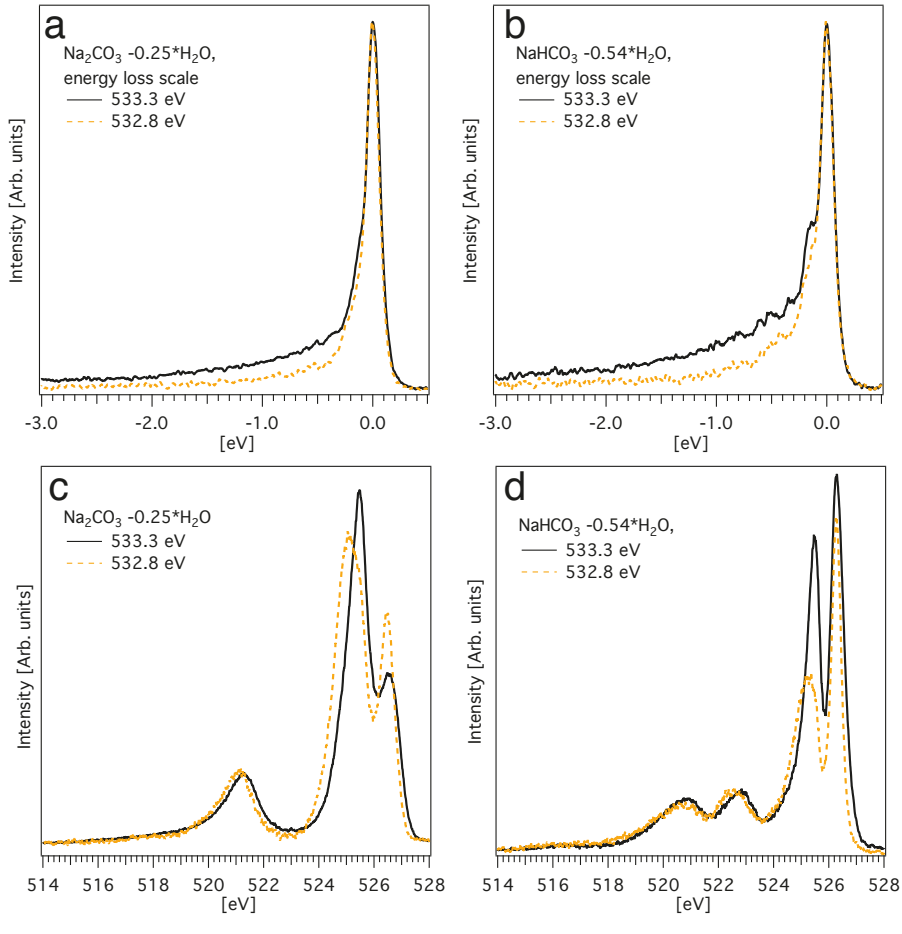

Figure 5.12. The water subtraction should be slightly different for the two energies though have been approximated to be the same. For the two solutions the water subtraction is almost the double in $NaHCO_3$ as expected since the concentration is half of the Na_2CO_3 solution.

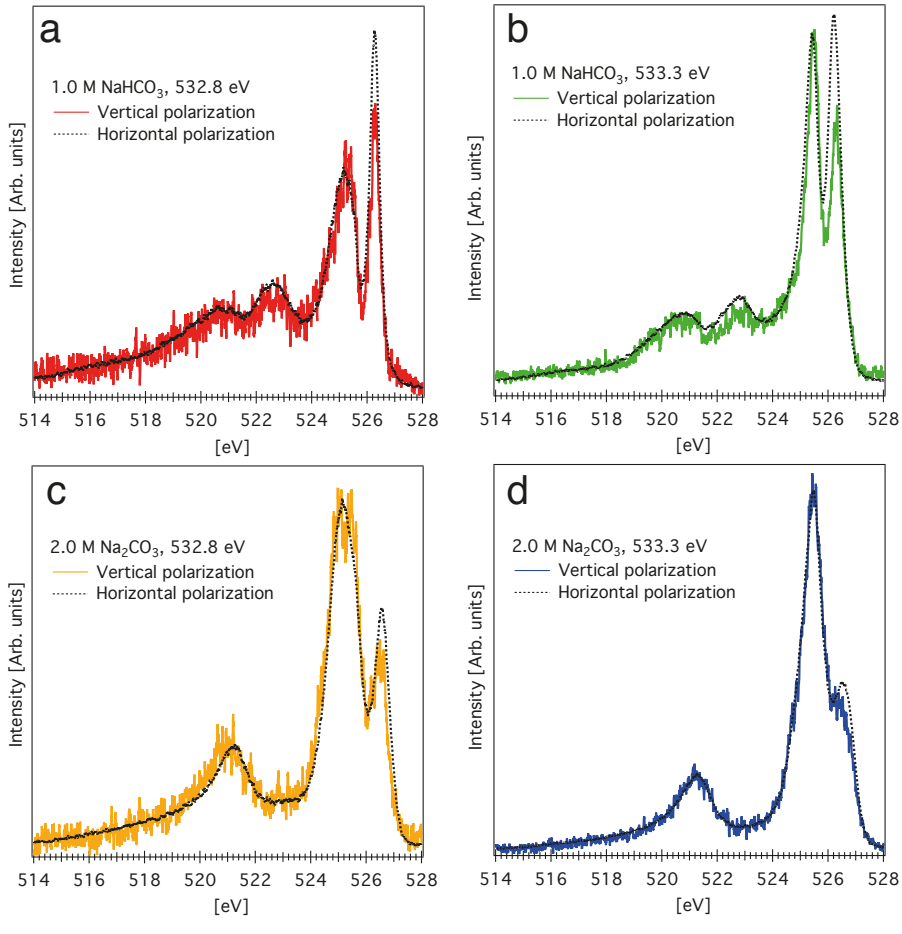

Figure 5.13. Note that water subtraction was not made for these spectra since no water spectra at vertical polarization were recorded.

6. Conclusions and Outlook

In this thesis I have investigated a number of aqueous solutions containing organic solutes related to atmospheric science. In particular, the surfaces of these solutions have been studied with the surface and chemical sensitive technique X-ray photoelectron spectroscopy. By comparing the surface signals, binding energy shifts and spectral ratios information about surface enrichments, interactions and orientation at the surface have been acquired. In paper I, the surface abundance of the guanidinium cation in a solution with Cl^- have been compared to solutions with added NaCl or Na_2SO_4 salts. Due to hydration competition, the surface propensity of guanidinium increased in the case with NaCl added but decreased when Na_2SO_4 was added. This was quite surprising since the doubly charged SO_4^{2-} anion is normally efficient at pushing other substances to the surface. This was explained by ion-paring between SO_4^{2-} and guanidinium – leading to conclusions that, even if this is a special case, salts might not always push other substances to the surface but can even do the opposite. In paper II another system displaying ion pairing is analyzed. Here two atmospherically relevant organic ions (hexylammonium and hexanoate) are studied one by one and in mixture. Even if both species are surface enriched in the single solute solutions they are even more surface enriched in the mixed solute solution. This was explained by three effects; ion pairing between the two charged head groups of the two organic compounds, van der Waals interactions between the alkyl chains and hydrophobic expulsion from the water of the alkyl chains . These three effects are believed to lead to a structural configuration where the ions either assembles in clusters or chains where the alkyl chain points out of the surface. This could be interesting for atmospheric science since even small concentrations of these, and perhaps similar compounds could lead to a very organic enriched water droplet surface. Through paper III-V, the surface enrichment and orientation at the surface of alcohols and two organic ions from paper II are probed. For these systems the surface concentration increases but saturates at some point with increasing bulk concentration. Specifically, a Langmuir isotherm adsorption model was applied to explain the surface saturation process. From this model Gibb's free energy of surface adsorption (ΔG_{Ads}) for these compounds were extracted, i.e. the difference in free energy for the system to bring the solute from the surface to the bulk. A gradual change in the orientation of the organic solutes were also observed for the compound with longer alkyl chains, were the chains point more and more out of the surface towards the vacuum as the surface got more crowded. This structural configuration facilitates for a higher

surface concentration. Interestingly the ΔG_{Ads} seems to change linearly with the number of carbons in the alkyl chain for the alcohols and the trend seems to be similar for compounds with other head groups. In paper III a building block model is proposed and if further investigations would confirm our suspicion the model could in the best case be used to predict ΔG_{Ads} values for compounds with several head groups. Paper VI takes on to investigate atmospherically relevant organic acids/bases by changing the pH value of the bulk and investigate the acid/base speciation at the surface. What at first seemed like a shift in the pH or pK_a values at the surface is instead explained by a non-equal surface enrichment of the acid and conjugated base. The (charge wise) neutral compound is more surface enriched compared to the charged one due to differences in hydration strength. This effect is seemingly more important than possible differences in pH or pK_a. This could also have consequences for atmospheric modeling since pH values are tricky to measure for atmospheric droplets. The RIXS studies in paper VII shows dramatic spectral changes for carbonate and bicarbonate with detuning at the O K-edge resonance. Polarization dependence was also noted for the HOMO, though further analysis is needed and the intriguing results justifies new measurements with higher resolution.

If one is allowed to speculate in how the work in this thesis could be used in the future and further development, I would start to advocate the community to continue with XPS studies as the technique along with MD simulations have shown to be quite useful to understand surface-bulk equilibra and consequential changes in surface structures. The next natural step would be to further investigate if and how ΔG_{Ads} varies with alkyl chains length for other compounds than alcohols and try out if the model holds for compounds with more than one head group. This would take a tremendous amount of beamtime to realize. One solution to this problem, if one is allowed to dream on technical development, might be a well controlled setup for in situ gradual dilution for liquid jet measurements. This could, in the best-case scenario, allow for measuring a full Langmuir adsorption curve in one go. To make a full concentration and pH variation map to further investigate the acid/base speciation in more complex solutions (as the one in paper II) and zwitter ions would also be very interesting. Even if the spectral overlap often is the limitation in mulicomponent samples the spectrometers are steadily getting better and truly ambient condition might used for more realistic experimental conditions.

The ultimate goal would of course to be properly describe the surface speciation in real atmospheric droplets – in the best of worlds this could help improve atmospheric models such that efficient methods could be developed to inhibit global warming so that future trekkers have the pleasure to experience the magnificent Bårddejiegna.

7. Populärvetenskaplig sammanfattning

När klimatforskare från World Weather Attribution-samarbetet nu fastslår att sannolikheten för extremväder ökar med vår mänskliga aktivitet på jorden bör vi lyssna – det är mycket som står på spel. Det är allmänt känt att koldioxid är en växhusgas liksom den mer potenta växhusgasen metan, vilket har låtit molnen falla i skugga. Moln, en samling av små vattendroppar eller aerosoler som de också kallas, bidrar faktiskt också till växhuseffekten. Dessa vattendroppar består självklart av vattenmolekyler, H_2O, men också av många andra molekyler och joner. Några av dessa förkommer naturligt, såsom olika typer av salter. Bordsalt, NaCl, förs till exempel upp från haven och lättflyktiga organiska molekyler från skogar. Det finns också ämnen såsom sot eller försurande substanser sprunget ur olika typer av industrier eller transporter. Vanligtvis är det en stor blandning av ämnen som till slut hamnar i de små vattendropparna, vilket gör det både klurigt men också intressant att reda ut hur de påverkar varandra både fysiskt och kemiskt.

Den här doktorsavhandlingen behandlar i första hand enkla modellsystem kopplade till atmosfärsvetenskap där också grundläggande ytfysiokemiska egenskaper har varit av intresse. Vattenytan är intressant av flera anledningar; för de små vattdropparna utgör just vattenytan en relativt stor del av volymen – vissa substanser är kraftigt anrikade just på ytan jämfört med vattnets innanmäte, den så kallade bulken. Extra intressant för just atmosfärsvetenskapen är att ytans komposition kan påverka vattendroppens förmåga att ta upp eller göra sig av med vatten.

Röntgenbaserad fotoemissionsspektroskopi, på engelska kallad X-ray Photoelectron spectrocopy (XPS) eller Electron Spectroscopy for Chemical Analysis (ESCA), är en ytkänslig metod som använts i den här avhandlingen. Med XPS kan en studera såväl fasta material, vätskor och gaser. Provet belyses med röntgenstålar, sedan mäts utgående elektroners hastigheter. Elektronerna sitter från början bundna i atomer men slits loss efter interaktionen med röntgenstålen. Det fiffiga med tekniken är att den utnyttjar det faktum att elektronerna sitter olika hårt bundna beroende på vilket atomslag de kommit ifrån. Det påvisas genom att beräkna skilladen i inkommande energi (från röntgenstålen) och utgående energi (från elektronernas hastighet). Det betyder att man kan avgöra vilket eller vilka ämnen som finns i provet. Vad som vid första anblick kan ses som en nackdel men är en av de stora styrkorna med XPS är att elektronerna kan krocka på vägen ut mot detektorn vilket gör det osannolikt att elektronerna som kommer från bulken av provet överhuvutaget flyr provet. Det betyder att de flesta elektronerna som detekteras kommer från ytan på provet.

Med hjälp av XPS och molekyldynamik-simuleringar beskriver första delen av avhandlingen hur en molekylär jon vid namn guanidnium (Gdm^+) med strukturen $(CH_2)_3N^+$ påverkas av andra joner i vattenlösning. Gdm^+ jonen är en funktionell grupp i aminosyran arginin men används också som en substans för att denaturera proteiner. Vissa substanser har en tendens att befinna sig i bulken stället för ytan och vice versa. Vanligtvis kommer substanser med laddning (joner), tendera att vara mer dragna till bulken på grund av vattenmolekylernas förmåga att bilda svaga elektriska fält på korta avstånd (dipolfält). Ju fler och högre koncentration av substanser i vattenlösningen blir desto högre blir också konkurrensen om att vara omgärdad av vattenmolekyler. I den här konkurrens-situationen blir vissa substanser tvingade till vattenytan till fördel för de substanser som är starkare bundna till vattnet. Genom att jämföra olika lösningar visar vi att Gdm^+ jonen blir ytanrikad när NaCl tillsätts, men oväntat nog bulkanrikad när Na_2SO_4 istället tillsätts. Särskilt förvånande är detta eftersom sulfatjonen (SO_4^{2-}) är känd för att vara extra bra på att konkurrera om vatten. Förklaringen visade sig ligga i att Gdm^+ och SO_4^{2-} attraheras av varandra och bildar ett så kallat jon-par och "dras ner" till bulken av SO_4^{2-} jonerna. Det här kan hjälpa till att förklara varför Gdm^+ jonen tappade sin förmåga att denaturera proteiner när SO_4^{2-} också fanns i samma lösning.

Den andra delen behandlar också jon-par men nu två organiska molekyler: hexylammonium ($CH_3(CH_2)_5NH_3^+$; $HexNH_3^+$) och
hexanoat ($CH_3(CH_2)_4COO^-$;$HexOO^-$). Syra-basparen av dessa organiska joner har visat sig finnas i vattendroppar vilket gör att det åtminstone finns en chans att det här modellsystemet skulle kunna påträffas i vattendroppar med ett pH-värde runt 7. Här jämfördes vattenlösningar med de organiska jonerna var för sig med blandningen av de båda. Det visade sig att de båda organiska jonerna var ytanrikade från början men blev ytterligare anrikade i blandningen. Vad som också observerades var att molylerna, som är raka, strukturerade om sig vid ytan så att kolkedjorna pekade ut ifrån ytan medan den laddade gruppen (NH_3^+, resp. COO^-) pekade inåt. Det observerades också en skillnad i hur hårt elektronerna satt bundna i de olika lösningarna. Det gav anledning till att göra simuleringar som inte bara bekräftade att de organiska jonerna bildade par utan även formade större strukturer eller kedjor. Då ytanrikningen är mycket kraftig i den blandade lösningen skulle resultaten kunna vara intressanta för liknande system med laddade organiska substanser förekommande i atomsfären.

Den tredje delen tittar faktiskt delvis på samma organiska joner, $HexOO^-$ och $HexNH_3^+$, men också alkoholer av olika kolkedjelängd. Här studerades substanserna var för sig men vid olika koncentrationer. Eftersom dessa substanser är naturligt ytanrikade blev deras yt-koncentration större ju större koncentration av substanserna i bulken blev. Jämfört med bulken är ytan ytterst begränsad och blir till slut mättad – vilket innebar att koncentrationen vid ytan därefter inte längre blev större med ökande bulk-koncentration. Precis som

tidigare ställer sig substanserna upp med sina kolkedjor, dels för att fler ska få plats, men också för att kolkedjorna inte gillar vatten (hydrofoba) utan föredrar att binda till varandra med van der Waals-interaktioner. Efter att ha jämfört substanser med olika kedjelängd och funktionella grupper ser det ut som att energin, som krävs för att en molekyl ska ta sig från ytan till bulken, verkar skala linjärt med antalet kol i kolkedjan. Detta kan eventuellt i framtiden användas för att förutsäga denna energi för andra, mer komplicerade, molekyler.

Den fjärde delen behandlar också den delvis samma molekyler som tidigare men analyserar dem och andra utifrån ett pH-perspektiv. pH-värdet är ett mått på hur surt eller basiskt en vattenlösning är och det har under en längre tid diskuterats hurvida pH-värdet på vattenytan skulle vara annorlunda jämfört med det i bulken. Trots tidigare försök med olika experimentella metoder och simuleringar har det givit motsägelsefulla resultat. De organiska substanserna som har studerats i fjärde delen är just syror och baser. Genom att ändra pH-värdet i bulken har vi kunnat mäta substansernas mängd på ytan vilket vid första anblick kan ses som ett mått på hur sur eller basiskt det är på ytan. Det visade sig att även om pH värdet eventuellt kan vara annorlunda på ytan verkar det som att det är än viktigare om den organiska basen eller syran är elektrisk laddad (jonisk). Detta kan förhoppningsvis vara till hjälp vid simuleringar av små vattendroppar, där pH-värdet är svårt att mäta.

I stort gör arbetet bakom avhandlingen små steg för att beskriva vissa specialfall som kan belysa viktiga mekanismer relevanta för biokemi och atmosfärsvetenskap men också ett försök att generalisera och beskriva mekanismerna bakom hur organiska substansers ytanrikning fungerar.

8. List of abbreviations

KE	kinetic energy
BE	binding energy
MD	molecular dynamics
XPS	X-ray photoelectron spectroscopy
$\mathbf{C}_{\alpha}$	alpha carbon, i.e. the carbon atom closes to the head group
$\mathbf{C}_{C}$	carbon atom in alkyl-chain
$\mathbf{Gdm}^{+}$	guanidinium cation
$\mathbf{HexNH}_3^{+}$	hexylammonium cation ($CH_3(CH_2)_5NH_3^+$)
$\mathbf{HexOO}^{-}$	hexanoate anion ($CH_3(CH_2)_4COO^-$)
$\Delta\mathbf{G}_{Ads}$	Gibb's energy of adsorption
n	sensitivity factor
g	surface enrichments factor
m	molal =mol/kg H_2O
M	molar = mol/dm^3
x_{bulk}	molar fraction in the bulk

9. Acknowledgments

First of all, huge thanks to my two super-supervisors Olle Björneholm and Jan-Erik Rubensson (Ruben). With Olle's constant support, which already started from the bachelor's diploma work, through my master's degree and now finally in these last five years, it has been a true learning experience and journey. In many aspects, Olle is the one responsible for why you are reading this text. By feeding my excitement with interesting projects and continuously inviting me as an unexperienced student to participate in actual(!) experiments at the synchrotron facility MAX-lab was absolutely crucial for me to continue on the road towards becoming a PhD student. I hope this is something you will continue with so that others will have the same opportunity. Ruben, whom I started to learn better during my PhD studies, has the astonishing skill to always be there for interesting discussions, new ideas and an almost endless supply of positivity. Thanks!

I would also like to thank the many coworkers and students in the XPS group during the years like Gunnar, Josephina, Madeleine, Nicklas B. P., Johan S, Wandared, Niklas O., Winwin, Clara, Isaak, Geethanjali and the many students over the years. Especially Gunnar, whom I, almost as the inquisitor himself, asked about the function of I411's parts down to almost every single washer, bolt and nut. Big thanks to you Josephina for pushing the field even further and teaching me a lot about how be systematic and navigate through the PhD studies. It was great fun during all the beamtimes! Madeleine, I don't know if it is with dread or gratitude I open a manuscript with your comments – I'm very grateful for your very thorough work!

Even though I didn't add many of the RIXS-results to this thesis there are projects in the pipeline that I still would like to thank the RIXS group for; Conny and Johan for learning me both practical and theoretical aspects of RIXS but also for all the help during the fun beamtimes, Minjie for the interesting philosophical and physics discussions, and of course also Marcus, Èva, Deepak and Ludde.

I would also like to thank the many german speaking officemates during the years; Josephina, Melanie, Madeleine, Corina, Felix, Clara, Isaak – you have hindered the worst decline of my poor german-skills but also enlightened me in the concepts of ringbahnsaufen und the "propper" way of pronouncing Käse among other things - Vielen Dank!

Thank you Molecular and Condensed Matter Physics – it has been a fun and rather long time (about 24% of my life as of today). During fika, lunches and seminars you have shared interesting facts, fun stories and forced me to spend my daily Google-moment[1] way to early. As some of you know, I have also enjoyed teaching and I would like to thank everyone that have shared the struggle of explaining fictitious forces, RLC-circuits and Bell's inequality to the students. Special thanks to Nic and Håkan who gave me the opportunity to hold lessons – that was both challenging and great fun!

I'm grateful for all the collaborators during the years for doing calculations, inviting me to beamtimes, projects and interesting discussions. Special thanks to Uppsala people Calle and Cecilia, the brazilians Arnaldo and Ricardo, former members of Pavel's Prague group such as Mario, Erik, Philip and Pavel himself, Harada group in Japan, sextant-beamline related people, Annette, Michael and Faris in Stockholm and the rest which I have not mentioned in name but absolutely deserve my gratitude!

Without the synchrotron facilities MAX-lab (now MAXIV), Bessy, SLS, Soleil, LNLS and SPring-8 there would have been no X-rays for all the projects I have been involved with! Thanks for the many photons and the supportive staff – especially MAX-lab where I have spent most of my beamtimes. They even provided me with semlor for two consecutive fettisdagar, significantly improving those night shifts.

Thank you reader or potential reader for picking up this thesis – I hope you find some of the results intriguing.

Tack kära stora familj, familía och vänner, ni betyder mycket för mig och har på olika sätt hjälpt mig under årens lopp – tack! P.S. Om ni nån gång ska skriva en avhandling – hör av er till mig, jag har några tips!

[1] Definition: a Google-moment is a single moment during a day that is available for googling trivia that potentially could ruin a speculative and interesting discussion.

References

[1] D. Koch and A. D. Del Genio. *Atmospheric Chemistry and Physics*, 10(16):7685–7696, aug 2010.

[2] T. Stocker, D. Qin, G. Plattner, and M. Tignor. *Climate Change 2013: The Physical Science Basis*. Cambridge University Press, 2013.

[3] Pavel Jungwirth and Douglas J. Tobias. *The Journal of Physical Chemistry B*, 106(25):6361–6373, 2002.

[4] Poul B. Petersen and Richard J. Saykally. *Annual Review of Physical Chemistry*, 57(1):333–364, 2006.

[5] N. L. Prisle, N. Ottosson, G. Öhrwall, J. Söderström, M. Dal Maso, and O. Björneholm. *Atmos. Chem. Phys.*, 12(24):12227–12242, dec 2012.

[6] Josephina Werner, Jan Julin, Maryam Dalirian, Nønne L. Prisle, Gunnar Öhrwall, Ingmar Persson, Olle Björneholm, and Ilona Riipinen. *Phys. Chem. Chem. Phys.*, 16:21486–21495, 2014.

[7] Ming-Tao Lee, Fabrizio Orlando, Luca Artiglia, Shuzhen Chen, and Markus Ammann. *J. Phys. Chem. A*, 120(49):9749–9758, 2016.

[8] Niklas Ottosson, Erik Wernersson, Johan Söderström, Wandared Pokapanich, Susanna Kaufmann, Svante Svensson, Ingmar Persson, Gunnar Öhrwall, and Olle Björneholm. *Phys. Chem. Chem. Phys.*, 13(26):12261, 2011.

[9] Yousung Jung and R. A. Marcus. 2007.

[10] Orlando Acevedo and Kira Armacost. *Journal of the American Chemical Society*, 132(6):1966–1975, feb 2010.

[11] Kevin R. Wilson, R. D. Schaller, D. T. Co, R. J. Saykally, Bruce S. Rude, T. Catalano, and J. D. Bozek. *The Journal of Chemical Physics*, 117(16):7738–7744, oct 2002.

[12] Niklas Ottosson, Knut J. Børve, Daniel Spångberg, Henrik Bergersen, Leif J. Säthre, Manfred Faubel, Wandared Pokapanich, Gunnar Öhrwall, Olle Björneholm, and Bernd Winter. *Journal of the American Chemical Society*, 133(9):3120–3130, 2011.

[13] Aderson Miranda da Silva, Alexandra Mocellin, Susanna Monti, Cui Li, Ricardo R. T. Marinho, Aline Medina, Hans Agren, Vincenzo Carravetta, and Arnaldo Naves de Brito. *The Journal of Physical Chemistry Letters*, 6(5):807–811, 2015. PMID: 26262656.

[14] Hans Siegbahn and Kai Siegbahn. *Journal of Electron Spectroscopy and Related Phenomena*, 2(3):319 – 325, 1973.

[15] M. Faubel, S. Schlemmer, and J. P. Toennies. *Zeitschrift für Physik D Atoms, Molecules and Clusters*, 10(2):269–277, Jun 1988.

[16] Hitoshi. Ohtaki and Tamas. Radnai. *Chemical Reviews*, 93(3):1157–1204, 1993.

[17] Richard Buchner, Ting Chen, and Glenn Hefter. *The Journal of Physical Chemistry B*, 108(7):2365–2375, 2004.

[18] Yizhak Marcus. *Chemical Reviews*, 109(3):1346–1370, 2009.

[19] Yizhak Marcus and Glenn Hefter. *Chem. Rev.*, 106(11):4585–4621, 2006. PMID: 17091929.
[20] Phillip L. Geissler, Christoph Dellago, and David Chandler. *The Journal of Physical Chemistry B*, 103(18):3706–3710, 1999.
[21] Nico F. A. van der Vegt, Kristoffer Haldrup, Sylvie Roke, Junrong Zheng, Mikael Lund, and Huib J. Bakker. *Chem. Rev.*, 116(13):7626–7641, 2016. PMID: 27153482.
[22] Nadia N. Casillas-Ituarte, Xiangke Chen, Hardy Castada, and Heather C. Allen. *The Journal of Physical Chemistry B*, 114(29):9485–9495, 2010. PMID: 20614879.
[23] L. Onsager and N. N. T. Samaras. *J. Chem. Phys.*, 2, 1934.
[24] Eva Brandes, Christiane Stage, Hubert Motschmann, Julian Rieder, and Richard Buchner. *The Journal of Chemical Physics*, 141(18):18C509, 2014.
[25] Lisa Götte, Krista M. Parry, Wei Hua, Dominique Verreault, Heather C. Allen, and Douglas J. Tobias. *The Journal of Physical Chemistry A*, 121(34):6450–6459, 2017. PMID: 28758749.
[26] Irving Langmuir. *Journal of the American Chemical Society*, 54(7):2798–2832, 1932.
[27] Poul B. Petersen and Richard J. Saykally. *Chemical Physics Letters*, 458(4):255 – 261, 2008.
[28] Robert M. Onorato, Dale E. Otten, Richard J. Saykally, and James L. Skinner. *Proceedings of the National Academy of Sciences of the United States of America*, 106(36):15176–15180, 2009.
[29] Kathryn A. Perrine, Marijke H. C. Van Spyk, Alexandria M. Margarella, Bernd Winter, Manfred Faubel, Hendrik Bluhm, and John C. Hemminger. *The Journal of Physical Chemistry C*, 118(50):29378–29388, 2014.
[30] M.-M. Walz, C. Caleman, J. Werner, V. Ekholm, D. Lundberg, N. L. Prisle, G. Öhrwall, and O. Björneholm. *Phys. Chem. Chem. Phys.*, 17(21):14036–14044, 2015.
[31] M-M Walz, J Werner, V Ekholm, N L Prisle, G Öhrwall, and O Björneholm. *Phys. Chem. Chem. Phys.*, 18(9):6648–6656, 2016.
[32] Patrick G. Grant, Shawna L. Lemke, Maxene R. Dwyer, and Timothy D. Phillips. *Langmuir*, 14(15):4292–4299, 1998.
[33] S. Hüfner. *Photoelectron Spectroscopy*. Springer-Verlag, 1995.
[34] J. Stöhr. *NEXAFS spectroscopy*. Springer-Verlag, 1992.
[35] Niklas Ottosson, Manfred Faubel, Stephen E. Bradforth, Pavel Jungwirth, and Bernd Winter. *Journal of Electron Spectroscopy and Related Phenomena*, 177(2):60 – 70, 2010. Water and Hydrogen Bonds.
[36] M. Bässler, J-.O. Forsell, O. Björneholm, R. Feifel, M. Jurvansuu, S. Aksela, S. Sundin, S.L. Sorensen, R. Nyholm, A. Ausmees, and S. Svensson. *J. Electron Spectrosc. Relat. Phenom.*, 101:953–957, 1999.
[37] M. Bässler, A. Ausmees, M. Jurvansuu, R. Feifel, J.-O. Forsell, P. de Tarso Fonseca, A. Kivimäki, S. Sundin, S.L. Sorensen, R. Nyholm, O. Björneholm, S. Aksela, and S. Svensson. *Nucl. Instrum. Methods Phys. Res., Sect. A*, 469(3):382–393, 2001.
[38] J. Cooper. *J. Chem. Phys.*, 48(2):942, 1968.

[39] Faris Gel'mukhanov and Hans Ågren. *Physics Reports*, 312(3-6):87–330, may 1999.
[40] Jan-Erik Rubensson. *Journal of Electron Spectroscopy and Related Phenomena*, 110-111:135 – 151, 2000. Soft X Ray Emission Spectroscopy.
[41] Akio Kotani and Shik Shin. *Rev. Mod. Phys.*, 73:203–246, Feb 2001.
[42] P. Salek, A. Baev, F. Gel'mukhanov, and H. Ågren. *Phys. Chem. Chem. Phys.*, 5:1–11, 2003.
[43] S. H. Southworth, D. W. Lindle, R. Mayer, and P. L. Cowan. *Phys. Rev. Lett.*, 67:1098–1101, Aug 1991.
[44] Giuseppe Graziano. *Phys. Chem. Chem. Phys.*, 13:12008–12014, 2011.
[45] Sven Heiles, Richard J. Cooper, Matthew J. DiTucci, and Evan R. Williams. *Chem. Sci.*, 6(6):3420–3429, 2015.
[46] Gunnar Öhrwall, Nønne L. Prisle, Niklas Ottosson, Josephina Werner, Victor Ekholm, Marie-Madeleine Walz, and Olle Björneholm. *J. Phys. Chem. B*, 119(10):4033–4040, mar 2015.
[47] J.A. Riddick, W.B. Bunger, and T.K. Sakano. *Techniques of Chemistry 4th ed., Volume II. Organic Solvents*. NY: John Wiley and Sons, New York, 1985.
[48] Y. You, V. P. Kanawade, J. A. De Gouw, A. B. Guenther, S. Madronich, M. R. Sierra-Hernández, M. Lawler, J. N. Smith, S. Takahama, G. Ruggeri, A. Koss, K. Olson, K. Baumann, R. J. Weber, A. Nenes, H. Guo, E. S. Edgerton, L. Porcelli, W. H. Brune, A. H. Goldstein, and S. H. Lee. *Atmospheric Chemistry and Physics*, 14(22):12181–12194, 2014.
[49] Sina Kummer, Wolfgang Ruth, and Udo Kragl. *Electroanalysis*, 28(9):1992–1999, 2016.
[50] Hua Chen, Wei Gan, Rong Lu, Yuan Guo, and Hong-fei Wang. *The Journal of Physical Chemistry B*, 109(16):8064–8075, 2005. PMID: 16851942.
[51] Ricardo R. T. Marinho, Marie-Madeleine Walz, Victor Ekholm, Gunnar Öhrwall, Olle Björneholm, and Arnaldo Naves de Brito. *The Journal of Physical Chemistry B*, 121(33):7916–7923, 2017. PMID: 28715892.
[52] P. Muller. *Pure Appl. Chem.*, 66:1077–1184.
[53] Y. Horikawa, A. Yoshida, O. Takahashi, H. Arai, T. Tokushima, T. Gejo, and S. Shin. *Journal of Molecular Liquids*, 189:9–12, 2014.
[54] Naohiro Nishida, Yuka Horikawa, Takashi Tokushima, and Osamu Takahashi. *Journal of Electron Spectroscopy and Related Phenomena*, 220:96–100, 2017.
[55] Hui Wen, Gao-Lei Hou, Yi-Rong Liu, Xue-Bin Wang, and Wei Huang. *Phys. Chem. Chem. Phys.*, 18:17470–17482, 2016.

Acta Universitatis Upsaliensis

Digital Comprehensive Summaries of Uppsala Dissertations from the Faculty of Science and Technology 1715

Editor: The Dean of the Faculty of Science and Technology

A doctoral dissertation from the Faculty of Science and Technology, Uppsala University, is usually a summary of a number of papers. A few copies of the complete dissertation are kept at major Swedish research libraries, while the summary alone is distributed internationally through the series Digital Comprehensive Summaries of Uppsala Dissertations from the Faculty of Science and Technology. (Prior to January, 2005, the series was published under the title "Comprehensive Summaries of Uppsala Dissertations from the Faculty of Science and Technology".)

Distribution: publications.uu.se
urn:nbn:se:uu:diva-357369

ACTA
UNIVERSITATIS
UPSALIENSIS
UPPSALA
2018